Development 139, 1806-1820 (2012) doi:10.1242/dev.077461

Functional interactions between Fat family cadherins in tissue morphogenesis and planar polarity

Sakura Saburi[1,*], Ian Hester[1], Lisa Goodrich[2] and Helen McNeill[1,3,*]

SUMMARY

The atypical cadherin *fat* (*ft*) was originally discovered as a tumor suppressor in *Drosophila* and later shown to regulate a form of tissue patterning known as planar polarity. In mammals, four *ft* homologs have been identified (*Fat1-4*). Recently, we demonstrated that *Fat4* plays a role in vertebrate planar polarity. *Fat4* has the highest homology to *ft*, whereas other Fat family members are homologous to the second *ft*-like gene, *ft2*. Genetic studies in flies and mice imply significant functional differences between the two groups of Fat cadherins. Here, we demonstrate that Fat family proteins act both synergistically and antagonistically to influence multiple aspects of tissue morphogenesis. We find that *Fat1* and *Fat4* cooperate during mouse development to control renal tubular elongation, cochlear extension, cranial neural tube formation and patterning of outer hair cells in the cochlea. Similarly, *Fat3* and *Fat4* synergize to drive vertebral arch fusion at the dorsal midline during caudal vertebra morphogenesis. We provide evidence that these effects depend on conserved interactions with planar polarity signaling components. In flies, the transcriptional co-repressor Atrophin (Atro) physically interacts with Ft and acts as a component of Fat signaling for planar polarity. We find that the mammalian orthologs of *atro*, *Atn1* and *Atn2l*, modulate *Fat4* activity during vertebral arch fusion and renal tubular elongation, respectively. Moreover, *Fat4* morphogenetic defects are enhanced by mutations in *Vangl2*, a 'core' planar cell polarity gene. These studies highlight the wide range and complexity of Fat activities and suggest that a Fat-Atrophin interaction is a conserved element of planar polarity signaling.

KEY WORDS: Fat cadherins, Atrophin, Cystic kidney disease, Mouse development, Planar polarity

INTRODUCTION

Proper coordination of tissue patterning and growth is essential for development of multicellular organisms. Genetic studies in *Drosophila melanogaster* revealed a crucial role for the cell adhesion molecule Fat (Ft) in regulating both tissue growth and a form of tissue organization known as planar polarity (Lawrence et al., 2008; Matakatsu and Blair, 2004; Yang et al., 2002). Effects on planar polarity are mediated by a signaling module, comprising the atypical cadherins Ft and Dachsous (Ds) and the kinase Four-jointed (Fj), that lies upstream of, or in parallel to, the 'core' planar cell polarity (PCP) elements, such as Frizzled (Fz), Dishevelled (Dvl, or Dsh) and Van Gogh (Vang), and tissue-specific effectors such as RhoA and Inturned (Axelrod, 2009; Goodrich and Strutt, 2011; Gray et al., 2011; Lawrence et al., 2008; Saburi and McNeill, 2005). Core PCP elements and tissue-specific effectors are conserved from flies to humans and are required for tissue organization in mice, including the polarized orientation of sensory hair cells in the cochleae and of hair follicles in the skin (Guo et al., 2004; Montcouquiol et al., 2003; Qian et al., 2007; Wang, J. et al., 2006) as well as convergent extension (CE) movements that occur during gastrulation, cochlear extension and neural tube closure (Axelrod, 2009; Goodrich, 2008; Simons and Mlodzik, 2008). How the Ft signaling module influences these events remains poorly understood.

Recently, we demonstrated that a mammalian homolog of *Drosophila ft*, *Fat4*, plays a fundamental role in vertebrate planar polarity (Saburi et al., 2008). Planar polarity is the organization of cells within the plane of a tissue, as exemplified by the orderly arrangement of sensory hair cells in the cochlea and by the coordinated movement of cells during CE. *Fat4*$^{-/-}$ mice display distinctive planar polarity phenotypes, including misorientation of hair cells, a short anterior-posterior body axis, short cochlear ducts and broadened spinal cord. Loss of *Fat4* also randomizes oriented cell division within renal tubular epithelia in the developing kidney, resulting in cystic kidney disease. Mutating one copy of *Vangl2*, a homolog of *Drosophila Vang*, significantly increased the severity of cystic tubular dilation in *Fat4*$^{-/-}$ kidneys. Furthermore, a murine homolog of *Drosophila ds*, dachsous 1 (*Dchs1*), functions with *Fat4* to control tissue patterning (Mao et al., 2011). These findings imply that the Ft/Ds/Fj signaling module might be conserved from flies to humans and that it acts in parallel to a *Vangl2*-dependent 'core' PCP pathway to ensure proper tissue morphogenesis and patterning.

The Fat family of cadherins comprises two family members in *Drosophila* (*ft* and *ft2*) and four in vertebrates (*Fat1-4*) (Tanoue and Takeichi, 2005). *Fat4* exhibits the highest homology to *ft*, whereas *Fat1* and *Fat3* are more similar to *ft2* [also called *kugelei* or *fat-like* (*ftl*)] (Castillejo-Lopez et al., 2004; Gutzeit et al., 1991). Loss of *ft2* in flies results in collapse of tracheal epithelia (Castillejo-Lopez et al., 2004). In contrast to *ft*, *ft2* mutations do not affect planar polarity in eyes and wings or induce hyperplastic overgrowth in imaginal discs. Instead, *ft2* mutant flies lose planar alignment of stress fibers in ovarian follicle cells (Viktorinova et al., 2009). These observations indicate significant functional differences between *ft* and *ft2* in flies. Similarly, *Fat1*$^{-/-}$ mice do not display planar polarity phenotypes or hyperplastic overgrowths (Ciani et al., 2003). Instead, *Fat1* mutants suffer from perinatal lethality accompanied by a failure in glomerular slit formation in kidneys. *Fat2*$^{-/-}$ and *Fat3*$^{-/-}$ mice also lack classic planar polarity phenotypes, with no discernible phenotypes reported in *Fat2*

[1]Samuel Lunenfeld Research Institute, Mount Sinai Hospital, Toronto, ON, M5G 1X5, Canada. [2]Department of Neurobiology, Harvard Medical School, Boston, MA 02115, USA. [3]Department of Molecular Genetics, University of Toronto, ON, M5S 1A1, Canada.

*Authors for correspondence (sakura.saburi@gmail.com; mcneill@lunenfeld.ca)

Accepted 27 February 2012

mutants (Barlow et al., 2010). The subcellular distribution of Fat3 in the nervous system suggests a role for Fat3 in neurite fasciculation (Mitsui et al., 2002; Nagae et al., 2007) and retinal cells in *Fat3*$^{-/-}$ mutants have altered dendritic morphology (Deans et al., 2011). Fat1 is proposed to control actin dynamics through interactions with Ena/Vasp proteins (Moeller et al., 2004; Tanoue and Takeichi, 2004). Thus, vertebrate orthologs of *Drosophila ft2* might function to regulate the cytoskeleton.

Most of what is known about Fat signaling pathways has come from analysis of flies. *Drosophila* Ft controls planar polarity and *fj* expression through interactions with the transcriptional co-repressor Atrophin (Atro; Grunge – FlyBase) (Fanto et al., 2003). Loss of *atro* leads to planar polarity defects in eyes and wings that phenocopy loss of *ft*. Moreover, *atro* mutant flies exhibit strong genetic interactions with *ft* in planar polarity. There are two human orthologs of *atro*: atrophin 1 (*ATN1*) and atrophin 2 (*ATN2*). *ATN2* encodes two alternative transcripts: *ATN2L* (also known as *RERE*) and *ATN2S* (Yanagisawa et al., 2000). ATN1 is a transcriptional co-activator (Shen et al., 2007), whereas ATN2L is a transcriptional co-repressor that recruits histone deacetylases (Zoltewicz et al., 2004). The human neurodegenerative disorder dentatorubral-phallidoluysian atrophy is caused by polyglutamine expansion in ATN1 (Yanagisawa et al., 2000). *Atn1* null mice have no overt phenotypes (Shen et al., 2007), whereas a truncated *Atn1t* allele impairs longevity and spermatogenesis (Yu et al., 2009). By contrast, *Atn2l* loss in ENU-induced *openmind* (*om*) mice leads to early embryonic lethality, with severe defects in ventralization of anterior neural plate, heart looping and somitogenesis (Zoltewicz et al., 2004). Fat1 and atrophins co-immunoprecipitate in smooth muscle and together regulate planar alignment of the microtubule-organizing center, directing polarized cell migration (Hou and Sibinga, 2009). Intriguingly, the transcriptional co-activator Atn1 potentiates these events, whereas the transcriptional co-repressor Atn2l inhibits migration.

To gain further insight into the role of Fat signaling during animal development, we asked whether different Fat family genes in mice have overlapping or redundant functions. To date, only *Fat4* has been implicated in planar polarity. One possibility is that vertebrate *ft*-like genes evolved distinct roles, similar to the functional separation of *ft* and *ft2* in flies. Alternatively, the action of Fat cadherins in planar polarity might be masked by their functional redundancies. We tested these hypotheses by exploring whether the distinctive phenotypes in *Fat4*$^{-/-}$ mutants would be modified by loss of *Fat1* or *Fat3*. We went on to investigate the molecular basis of Fat4 signaling in diverse morphogenetic contexts by testing genetic interactions with *Fjx1*, atrophins and *Vangl2*. Taken together, our genetic studies reveal complex synergistic and antagonistic interactions among Fat family genes, and suggest that Fat4 functions in atrophin-dependent pathways to direct tissue organization and planar polarity during mouse development.

MATERIALS AND METHODS

Mouse lines

The *Fat4*$^{2E11\Delta flox}$ allele (Saburi et al., 2008) was maintained by backcrossing to 129S3/SvImJ inbred mice (The Jackson Laboratory, USA). *Fat1*^{lacZneo} mice were a gift from Dr Charles ffrench-Constant (University of Edinburgh, UK). *Vangl2*^{Lp} (*Vangl2*^{S464N}) mice were generously provided by Dr Phillipe Gros (McGill University, Canada). *Fjx1*^{lacZ} were generously provided by Dr Manfred Gessler (University of Würzburg, Germany). *Atn1*$^{\Delta}$ and *Atn2*^{om} were generous gifts from Dr Andrew Peterson (Genentech, USA). Double heterozygotes were generated by crosses between heterozygous mice, and were maintained by backcrossing to 129S3/SvImJ.

Quantitative analysis of cystogenesis

Serial Hematoxylin and Eosin (H&E)-stained longitudinal sections of newborn kidney (4 μm) were prepared as described (Saburi et al., 2008). The entire slide (15-22 sections per kidney) was digitized with Aperio Scanner (Aperio Technologies), and sections were processed for quantification of luminal space with Image-Pro software (Media Cybernetics). For spatial filtering, the lower threshold was set to 50 μm^2. Sets of luminal space were summed and divided by total volume of kidney sections. To control for genetic background effects, all controls were obtained from siblings in the respective cross.

Analysis of inner ears

Inner ears were fixed in 4% paraformaldehyde for 24 hours at 4°C. After fixation, cochleae were incubated with anti-acetylated α-tubulin antibodies (Sigma) in PBS and/or anti-frizzled 6 (Fz6) antibodies (gift of Dr Jeremy Nathans, Johns Hopkins University, USA) as described (Saburi et al., 2008). Fluorescent images were processed for length analysis with Image-Pro software. The cochlea was divided into four regions defined as basal, mid-basal, mid-apical and apical turn. One continuous gain or loss of outer hair cell patches was counted as an emergence.

Quantification of the length of the mediolateral and dorsoventral axes of the vertebrae

H&E-stained transverse sections of newborn lumbar vertebra were prepared as described (Saburi et al., 2008). Images were processed for measurements of the distance between vertebral pedicles and between vertebral body and top roof of cartilaginous annulus (see Fig. 1E) with Image-Pro software. Primary numerical data and details of statistical analyses are available at www.mshri.on.ca/mcneill.

RESULTS

Morphogenetic anomalies caused by loss of *Fat4*

Fat4$^{-/-}$ mice exhibit a range of phenotypes consistent with defective planar polarity, including cystic kidneys, short cochleae and laterally broadened lumbar spinal cords (Saburi et al., 2008). In order to investigate whether other Fat family members and planar polarity signaling components influence Fat4 function in these tissues, we first performed a quantitative analysis of these phenotypes in *Fat4*$^{-/-}$ mutants. *Fat4*$^{-/-}$ kidneys exhibit multiple anomalies, including cystic dilations of renal tubules, reduced branching of the ureteric bud (UB) and a decrease in organ size (Mao et al., 2011; Saburi et al., 2008) (Fig. 1A,B). Cystic tubular dilations are prominent in *Fat4*$^{-/-}$ kidneys, especially in the loops of Henle and collecting ducts (Fig. 1A′,B′).

In *Fat4*$^{-/-}$ mutants, cochleae are small and malformed, with modest effects on vestibular apparatus size (supplementary material Fig. S1B,C). Morphometric analysis revealed that both cochleae (P=2.09×10^{-10}) and vestibules (P=4.93×10^{-3}) are significantly reduced in size (supplementary material Fig. S1F). However, the cochlea-to-vestibule ratio of *Fat4*$^{-/-}$ inner ears is significantly lower than that of wild-type siblings (P=5.57×10^{-8}; supplementary material Fig. S1G), indicating that loss of *Fat4* causes a reduction in the size of both the cochlear and vestibular apparatus, with a stronger impact in the cochleae. Indeed, the cochlea is consistently shorter in *Fat4*$^{-/-}$ mutants than in wild type (Saburi et al., 2008) (Fig. 1C′,D′), even after normalization to the vestibule (P=1.47×10^{-6}; supplementary material Fig. S1G). In addition, the base of the cochleae does not form the proper curvature (supplementary material Fig. S2A,C). These observations suggest that loss of *Fat4* results in reduction in cochlear length, which is likely to be due to a failure in elongation rather than to reduction in inner ear size. Although *Fat4*$^{-/-}$ newborns are considerably shorter than wild-type newborns (Saburi et al., 2008), they are comparable in body weight to wild-type or *Fat4*$^{-/+}$ siblings (supplementary material Fig. S3A). Therefore, the hypoplastic *Fat4*$^{-/-}$ inner ears are likely to result from defects in morphogenesis and not from overall growth retardation.

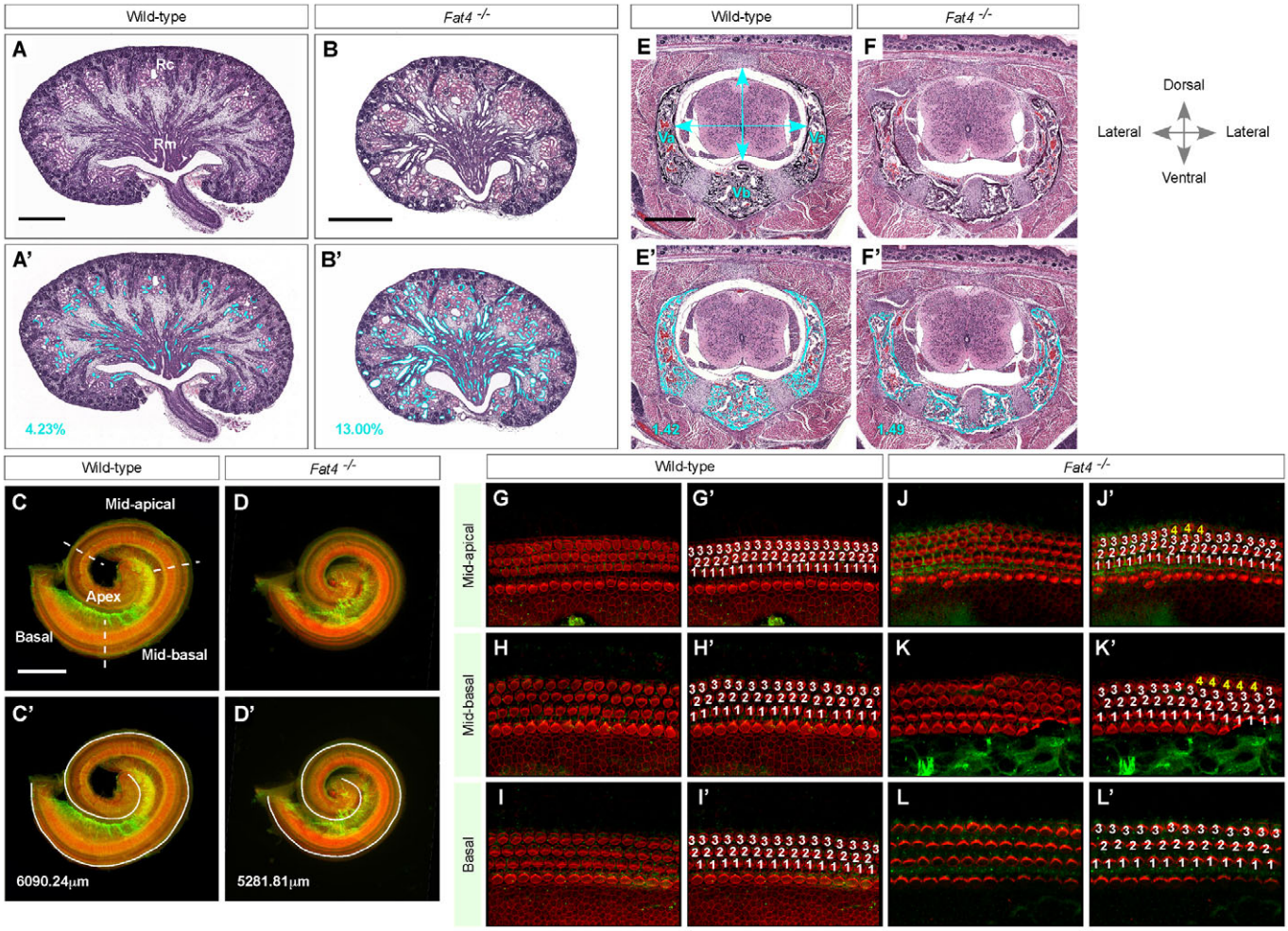

Fig. 1. Loss of *Fat4* alters the morphology of kidney, cochlea and caudal vertebra. (**A-B′**) H&E-stained sections of postnatal day (P) 0 wild-type (A) and *Fat4*$^{-/-}$ (B) mouse kidney. Dilated tubular lumens are outlined in light blue in the wild-type (A′) and *Fat4*$^{-/-}$ (B′) kidney. Percentages of luminal space relative to total volume of wild-type and *Fat4*$^{-/-}$ kidneys are reported in A′ and B′. Rc, renal cortex; Rm, renal medulla. (**C-D′**) Phalloidin-stained P0 cochlear epithelia from wild-type (C) and *Fat4*$^{-/-}$ (D) inner ear. Lengths of wild-type and *Fat4*$^{-/-}$ cochlea (white spiral lines) are indicated in C′ and D′. The sensory epithelium was divided into four domains (apex, mid-apical, mid-basal and basal turn) for quantitative analysis, as defined by the white dashed lines in C. (**E-F′**) H&E-stained transverse sections of a P0 wild-type (E) and *Fat4*$^{-/-}$ (F) lumbar vertebra. Vertebrae, composed of vertebral body (Vb) and vertebral arches (Va), are highlighted in light blue in wild type (E′) and *Fat4*$^{-/-}$ mutant (F′). Ratios of mediolateral axis (horizontal line) to dorsoventral axis (vertical line) in wild-type and *Fat4*$^{-/-}$ animals are reported in E′ (1.42) and F′ (1.49). Dorsal is up and lateral is to the right and left, here and in all subsequent figures. (**G-L′**) Immunofluorescence with antibodies against the kinocilium marker acetylated α-tubulin (green) and phalloidin staining of actin (red) on P0 wild-type (G,H,I) and *Fat4*$^{-/-}$ (J,K,L) cochlear sensory epithelia. Fluorescent images of mid-apical, mid-basal and basal turn are shown in the top, middle and bottom panels. The apex was not analyzed owing to low fidelity of hair cell patterning (Brooker et al., 2006). Outer hair cells (OHCs) are labeled by row number (1-3) in white (G′-L′), with discontinuous ectopic OHC4s (4) in yellow (J′,K′). Scale bars: 500 μm.

During cochlear development, one row of inner hair cells (IHCs) and three rows of outer hair cells (OHCs) are patterned with remarkable fidelity along the length of the organ of Corti (OOC) (Fig. 1G,H,I and supplementary material Fig. S3D). Loss of *Fat4* causes a modest misorientation of hair cells, predominantly in the third row OHCs (OHC3s) (Mao et al., 2011; Saburi et al., 2008). In addition, discontinuous extra rows of OHCs emerge in mid-apical and, more rarely, in mid-basal turns of *Fat4*$^{-/-}$ cochleae (Fig. 1J,K,L), in a fourth row, labeled OHC4s, that typically contains 3-10 cells (Fig. 1J′-L′).

Another site of *Fat4* activity is the caudal spinal cord, which is broadened laterally and flanked by vertebrae that are not fully developed and remain unfused upon loss of *Fat4* (Fig. 1E,F). The mediolateral vertebral length between the two pedicles is larger in *Fat4*$^{-/-}$ mutants than in wild-type siblings [mediolateral-to-dorsoventral (ML/DV) ratio of lumbar vertebra: wild-type 1.40±0.11 (n=30) versus *Fat4*$^{-/-}$ 1.62±0.13 (n=18); P=9.72×10^{-8}; compare Fig. 1F with 1E]. This is consistent with a recent report from Mao et al. (Mao et al., 2011) that vertebral column width is modestly increased in *Fat4*$^{-/-}$ mutants exclusively in the lumbar and posterior thoracic region.

Fat4 and Vangl2 synergize in diverse tissue morphogenesis

The kidney, cochlea and spinal cord phenotypes observed in *Fat4*$^{-/-}$ mutants are similar to those of *Looptail* (*Lp*) mutant mice. In flies, both Fat signaling and core PCP activity are required for planar polarity. Since most *Lp* phenotypes reflect disruptions in planar

polarity, *Fat4* and *Vangl2* might work together in vertebrate planar polarity. Most planar polarity phenotypes are more severe in *Vangl2 Lp* mutants than in $Fat4^{-/-}$ mutants (Montcouquiol et al., 2003), with the exception of the kidney (Yates et al., 2010). *Vangl2 Lp* mutants display modest anomalies in kidneys in terms of the cystic tubular dilations, UB branching and reduction in organ size that are typical of $Fat4^{-/-}$ mutants (compare supplementary material Fig. S4D,E; 129S3 background).

Cystic defects in $Fat4^{-/-}$ kidneys increase in severity upon introduction of one copy of the *Vangl2 Lp* mutation (Saburi et al., 2008) in a background of [(129P2/Ola × FVB/N)F1 × BCF1]F2. Exacerbation of cystic defects caused by the *Lp* mutation were consistent in a 129S3 background ($P=2.92\times10^{-3}$; Fig. 2C,D,P). $Vangl2^{Lp/+}$ heterozygotes do not exhibit obvious kidney anomalies on the 129S3 background (Fig. 2A,B), as demonstrated by quantifying the total dilated luminal space of tubules in the kidneys ($P=0.09$; Fig. 2P).

During inner ear development, the cochlear epithelium undergoes significant elongation mediated by CE movement (Yamamoto et al., 2009). In *Vangl2 Lp* mutants, defective PCP signaling disrupts CE and results in short and broad cochlear epithelium (Montcouquiol et al., 2003; Qian et al., 2007; Wang, J. et al., 2006). Although $Vangl2^{Lp/+}$ heterozygotes exhibit no change in cochlear length ($P=0.52$; Fig. 2E,F,Q), $Fat4^{-/-}$ cochlear elongation defects are significantly enhanced by the presence of a *Vangl2 Lp* mutation ($P=5.92\times10^{-5}$; Fig. 2G,H,Q). The vestibular apparatus of $Fat4^{-/-};Vangl2^{Lp/+}$ inner ears is externally comparable to that of $Fat4^{-/-}$ siblings (supplementary material Fig. S2J,K,M,N). Intriguingly, the distribution of Fz6 is not disrupted in the $Fat4^{-/-}$ OOC (supplementary material Fig. S5A′,B′). These findings suggest that *Fat4* cooperates with *Vangl2* to control cochlear elongation, but independently of the asymmetric subcellular distribution of the core PCP elements.

In addition to cochlear shortening, defects in CE during inner ear development frequently cause aberrant organization of hair cells in the OOC (Montcouquiol et al., 2003; Qian et al., 2007; Wang, J. et al., 2006). To determine whether *Fat4* and *Vangl2* also act together to pattern the sensory epithelium, we investigated whether the extra OHCs (OHC4s) seen in $Fat4^{-/-}$ cochleae increase in frequency upon introduction of a *Vangl2 Lp* mutation. Importantly, $Vangl2^{Lp/+}$ heterozygotes show no specific defects in the OOC (Fig. 2S). However, patches of OHC4s emerged more frequently in the mid-apical turn of $Fat4^{-/-};Vangl2^{Lp/+}$ cochleae than in $Fat4^{-/-}$ mutants ($P=7.54\times10^{-3}$; Fig. 2M,N,O,S). Moreover, ectopic OHC4s are often continuous exclusively in the mid-apical region of $Fat4^{-/-};Vangl2^{Lp/+}$ cochleae (Fig. 2S). Thus, synergy between *Fat4* and *Vangl2* influences both cochlear lengthening and patterning. The modest misorientation of hair cells in the $Fat4^{-/-}$ OOC is not detectably exacerbated upon introduction of a *Vangl2 Lp* mutation (Fig. 2M-O).

One of the most dramatic phenotypes observed in *Vangl2 Lp* mutants is craniorachischisis, characterized by anencephaly accompanied by spina bifida (Montcouquiol et al., 2003) (supplementary material Fig. S4E). The spinal cord and vertebral column are normal in $Vangl2^{Lp/+}$ newborns, indicating that there is no *Vangl2* haploinsufficiency in caudal neural tube and axial skeleton morphogenesis (ML/DV ratio of lumbar vertebra, $P=0.20$; Fig. 2I,J,R; data not shown). $Fat4^{-/-};Vangl2^{Lp/+}$ mutants are born without detectable malformations in the cranial neural tube (supplementary material Table S1). In addition, the presence of the *Vangl2 Lp* mutation did not consistently exacerbate $Fat4^{-/-}$ spinal cord or vertebral phenotypes (Fig. 2K,L,R; data not shown).

Synergy between Fat1 and Fat4 in kidney and cochlea morphogenesis

Many phenotypes observed in $Fat4^{-/-}$ mutants are modest compared with those of core PCP mutants, raising the possibility that *Fat4* functions in a redundant manner with other Fat family cadherins. To examine functional redundancies among Fat family members, we tested whether cystic defects in $Fat4^{-/-}$ kidneys increase in severity upon loss of one copy of *Fat1*. During kidney development, Fat1 is expressed in the UB epithelium (Rock et al., 2005). $Fat1^{-/-}$ kidneys do not exhibit visible dilations of renal tubules or reduction in organ size (supplementary material Fig. S4A,B), nor is there evidence for haploinsufficiency, as measured by quantification of total renal tubular luminal space ($P=0.88$; Fig. 3A,B,P). Strikingly, however, removal of one copy of *Fat1* significantly enhances cystic tubular dilations of $Fat4^{-/-}$ kidneys ($P=2.83\times10^{-2}$; Fig. 3C,D,P), with defects prominent in loops of Henle and collecting ducts (Fig. 3D).

To determine whether *Fat4* also synergizes with *Fat1* during cochlear elongation, we quantified $Fat4^{-/-}$ cochlea length in a $Fat1^{-/+}$ background. Although $Fat1^{-/-}$ homozygotes occasionally exhibit aberrant round ears (supplementary material Fig. S2A,B,E,F), no defects in cochlear lengthening were observed in $Fat1^{-/+}$ heterozygotes compared with wild type ($P=0.46$; Fig. 3E,F,Q). However, upon loss of one copy of *Fat1*, $Fat4^{-/-}$ cochleae became slightly shorter than in $Fat4^{-/-}$ mutants ($P=1.03\times10^{-2}$; Fig. 3G,H,Q).

Next, we asked whether synergy between *Fat1* and *Fat4* also governs patterning of OHCs. $Fat1^{-/+}$ heterozygotes show neither alterations of row numbers nor misorientations of hair cells in the OOC (Fig. 3S; data not shown). However, in $Fat1^{-/+};Fat4^{-/-}$ mutants the frequency of OHC4s increased in mid-basal and basal turns of cochleae ($P=1.37\times10^{-2}$ for the basal turn; Fig. 3M-O,S). Thus, removal of one copy of *Fat1* makes the OHC row number more sensitive to loss of *Fat4*. Notably, more than one extra row of OHCs was never observed in the $Fat1^{-/+};Fat4^{-/-}$ OOC (Fig. 3M,N,O).

Fat1 and *Fat4* are expressed in both the developing neural tube and intervertebral discs (Rock et al., 2005). However, $Fat1^{-/-}$ homozygotes revealed no apparent anomalies in spinal cord and vertebrae even in the lumbar region (ML/DV ratio of lumbar vertebra, $P=0.21$; Fig. 3I,J,R). Moreover, loss of *Fat1* did not alter the severity of either spinal cord or vertebral phenotypes in $Fat4^{-/-}$ mutants ($P=0.16$; Fig. 3K,L,R).

Synergy between Fat1 and Fat4 in cranial neural tube morphogenesis

Murine *ft*-like genes are also expressed in the developing neural tube, suggesting a role for Fat cadherins in neural tube morphogenesis (Rock et al., 2005). $Fat1^{-/-}$ mutants have deformed eyes and craniofacial malformations, with a low incidence of holoprosencephaly (Ciani et al., 2003). We found that $Fat1^{-/-}$ mutants born from $Fat1^{-/+};Fat4^{-/+}$ intercrosses in a (C57BL/6 × 129S3)F1 background often displayed exencephaly (supplementary material Table S2). On a 129S3 background, however, $Fat1^{-/-}$ mutants were born at the predicted Mendelian ratio, with no external anomalies other than facial malformations (Fig. 4F and supplementary material Table S3). These observations suggest that 129S3 restricts the incidence of exencephaly in $Fat1^{-/-}$ mutants, implying the existence of recessive modifier loci for *Fat1* in cranial neural tube development.

At 18.5 days of gestation (E18.5), three-quarters of $Fat1^{-/-};Fat4^{-/-}$ mutants were exencephalic (Fig. 4A,C-E), indicating synergy between Fat1 and Fat4 in cranial neural tube

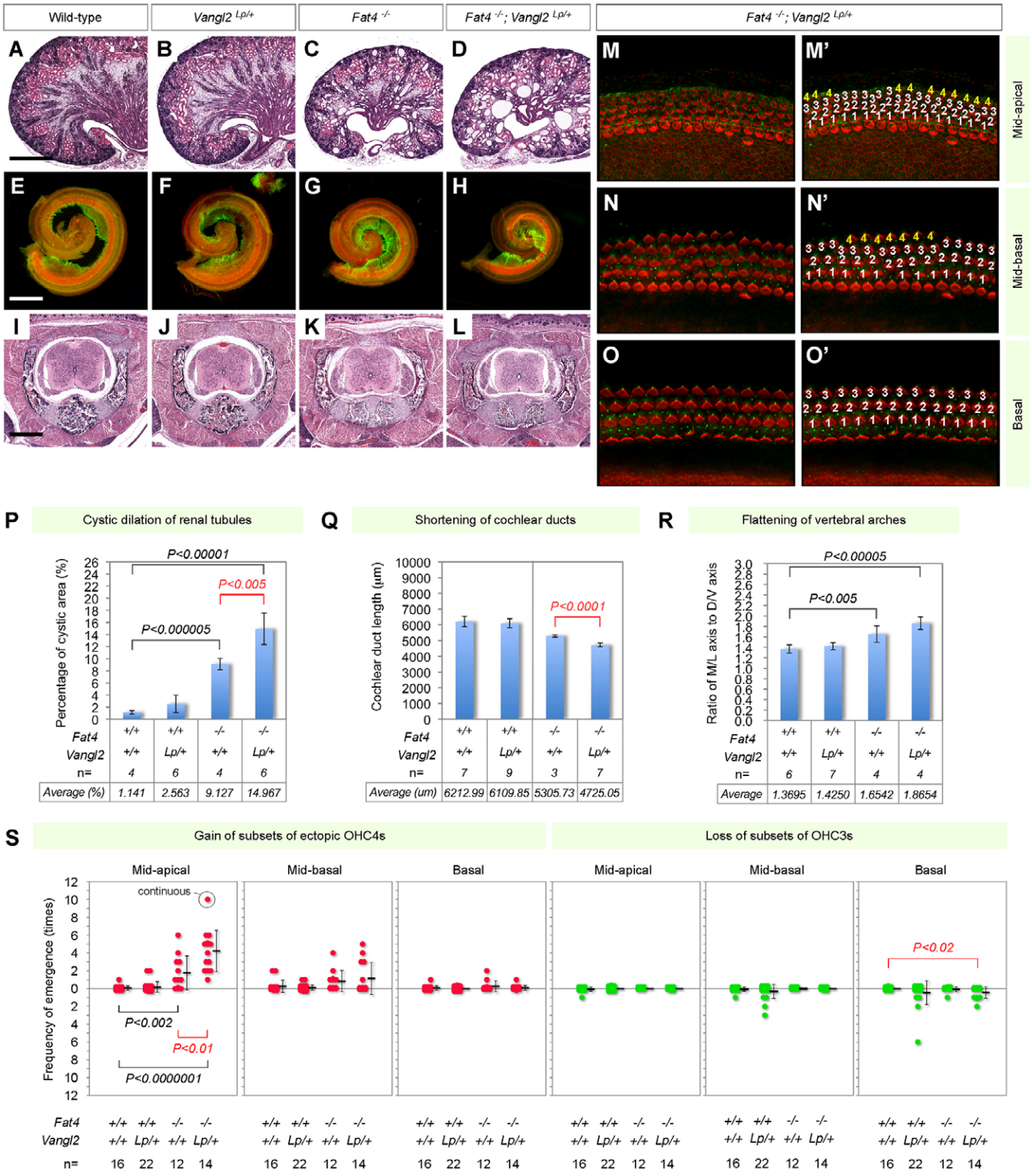

Fig. 2. *Vangl2* cooperatively interacts with *Fat4* in kidney, cochlea and caudal vertebra. (**A-D**) H&E-stained longitudinal sections of P0 wild-type (A), *Vangl2*$^{Lp/+}$ (B), *Fat4*$^{-/-}$ (C) and *Fat4*$^{-/-}$;*Vangl2*$^{Lp/+}$ (D) mouse kidney. (**E-H**) Phalloidin-stained cochlear epithelia of P0 wild type (E) and *Vangl2*$^{Lp/+}$ (F), *Fat4*$^{-/-}$ (G) and *Fat4*$^{-/-}$;*Vangl2*$^{Lp/+}$ (H) mutants. (**I-L**) H&E-stained transverse sections of P0 wild-type (I), *Vangl2*$^{Lp/+}$ (J), *Fat4*$^{-/-}$ (K) and *Fat4*$^{-/-}$;*Vangl2*$^{Lp/+}$ (L) lumbar vertebra. (**M-O'**) Immunofluorescence on *Fat4*$^{-/-}$;*Vangl2*$^{Lp/+}$ cochlear sensory epithelium as in Fig. 1G-L'. (**P-R**) Morphometric analyses of renal tubular dilation (P), cochlear shortening (Q) and vertebral arch broadening (R). Statistical analysis was by two-sample *t*-test assuming equal variances. Error bars indicate s.d. (**S**) Frequency plots of gain or loss of OHC patches in the OOC. Phenotypic severity was assessed by the frequency of emergence of ectopic OHC4s (red plots in left panels) or loss of OHC3s (green plots in right panels). Average frequency and s.d. are shown by horizontal and vertical black bars adjacent to the plot, respectively. Statistics was performed by analysis of variance (ANOVA). Scale bars: 500 μm.

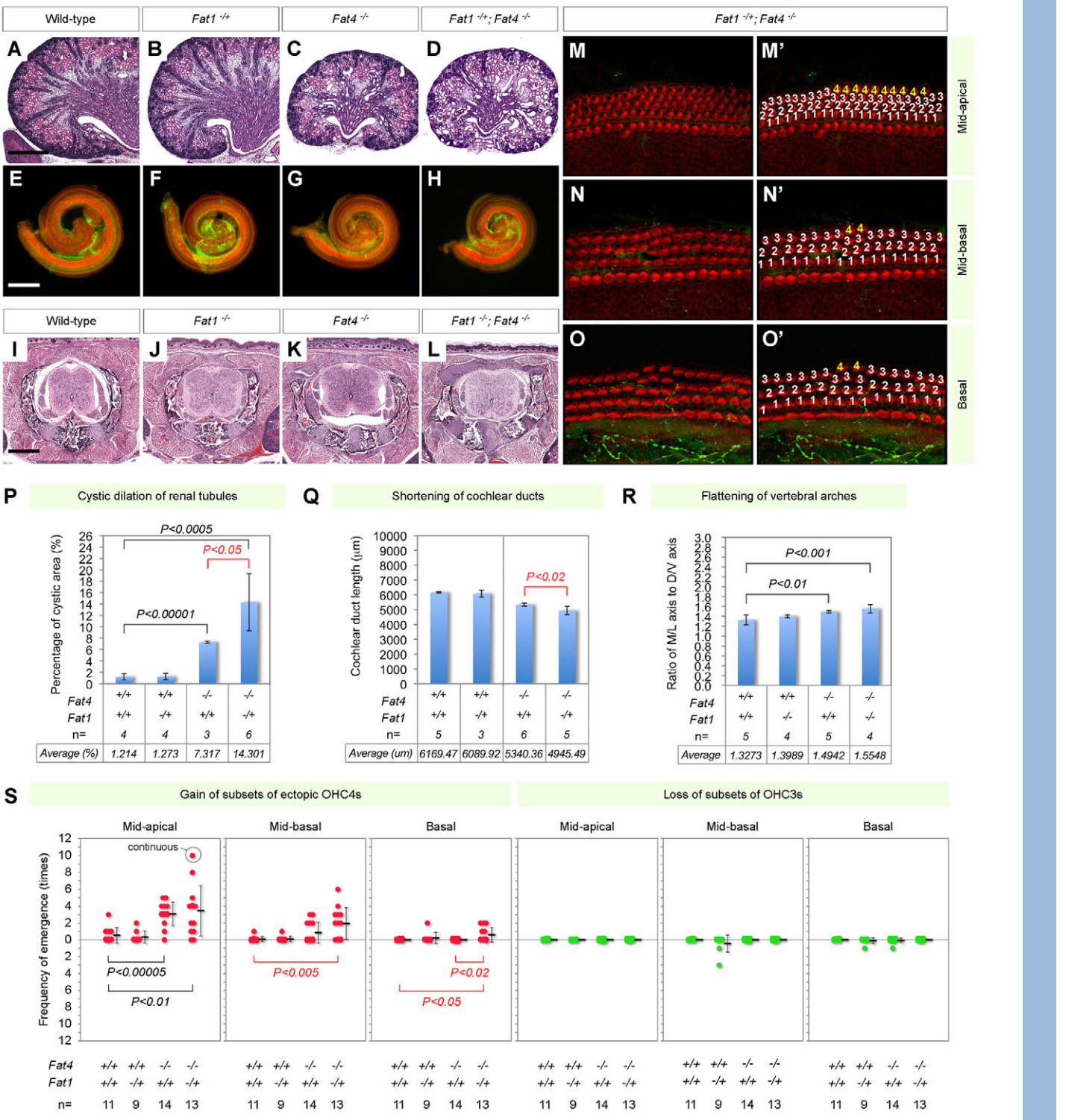

Fig. 3. *Fat1* synergizes with *Fat4* in kidney and cochlea. (**A-D**) H&E-stained longitudinal sections of P0 wild-type (A), *Fat1*$^{-/+}$ (B), *Fat4*$^{-/-}$ (C) and *Fat1*$^{-/+}$;*Fat4*$^{-/-}$ (D) mouse kidney. (**E-H**) Phalloidin-stained cochlear epithelia of P0 wild type (E) and *Fat1*$^{-/+}$ (F), *Fat4*$^{-/-}$ (G) and *Fat1*$^{-/+}$;*Fat4*$^{-/-}$ (H) mutants. (**I-L**) H&E-stained transverse sections of P0 wild-type (I), *Fat1*$^{-/+}$ (J), *Fat4*$^{-/-}$ (K) and *Fat1*$^{-/+}$;*Fat4*$^{-/-}$ (L) lumbar vertebra. (**M-O′**) Immunofluorescence on *Fat1*$^{-/+}$;*Fat4*$^{-/-}$ cochlear sensory epithelium as in Fig. 1G-L′. (**P-R**) Morphometric analyses of renal tubular dilation (P), cochlear shortening (Q) and vertebral arch broadening (R). Statistics performed as in Fig. 2P-R. (**S**) Frequency plots of gain or loss of OHC patches in the OOC. Phenotypic severities were defined and presented as in Fig. 2S. Scale bars: 500 μm.

development. The exencephalic *Fat1*$^{-/-}$;*Fat4*$^{-/-}$ embryos display cyanosis, indicating problems in the respiratory and/or blood circulation system. Notably, the double mutants exhibit swollen inner ears with extremely shortened and widened cochleae (Fig. 4N,O). Importantly, neither *Fat1*$^{-/-}$ nor *Fat4*$^{-/-}$ siblings exhibited cranial neural tube defects on this background (Fig. 4A,F).

A

Fat1 genetic interaction with *Fat4* in cranial neural tube formation

Genotype		Total number of embryos	Number of exencephalic embryos
Fat1 locus	*Fat4* locus		
Fat1 $^{+/+}$ or $^{-/+}$	*Fat4* $^{+/+}$ or $^{-/+}$	15	0 (0.0%)
Fat1 $^{-/-}$	*Fat4* $^{+/+}$ or $^{-/+}$	6	0 (0.0%)
Fat1 $^{+/+}$ or $^{-/+}$	*Fat4* $^{-/-}$	5	0 (0.0%)
Fat1 $^{-/-}$	*Fat4* $^{-/-}$	4	3 (75.0%)

B

Fat1 genetic interaction with *Fjx1* in cranial neural tube formation

Genotype		Total number of embryos	Number of anencephalic embryos
Fat1 locus	*Fjx1* locus		
Fat1 $^{+/+}$ or $^{-/+}$	*Fjx1* $^{+/+}$ or $^{-/+}$	39	0 (0.0%)
Fat1 $^{-/-}$	*Fjx1* $^{+/+}$ or $^{-/+}$	8	0 (0.0%)
Fat1 $^{+/+}$ or $^{-/+}$	*Fjx1* $^{-/-}$	12	0 (0.0%)
Fat1 $^{-/-}$	*Fjx1* $^{-/-}$	6	3 (50.0%)

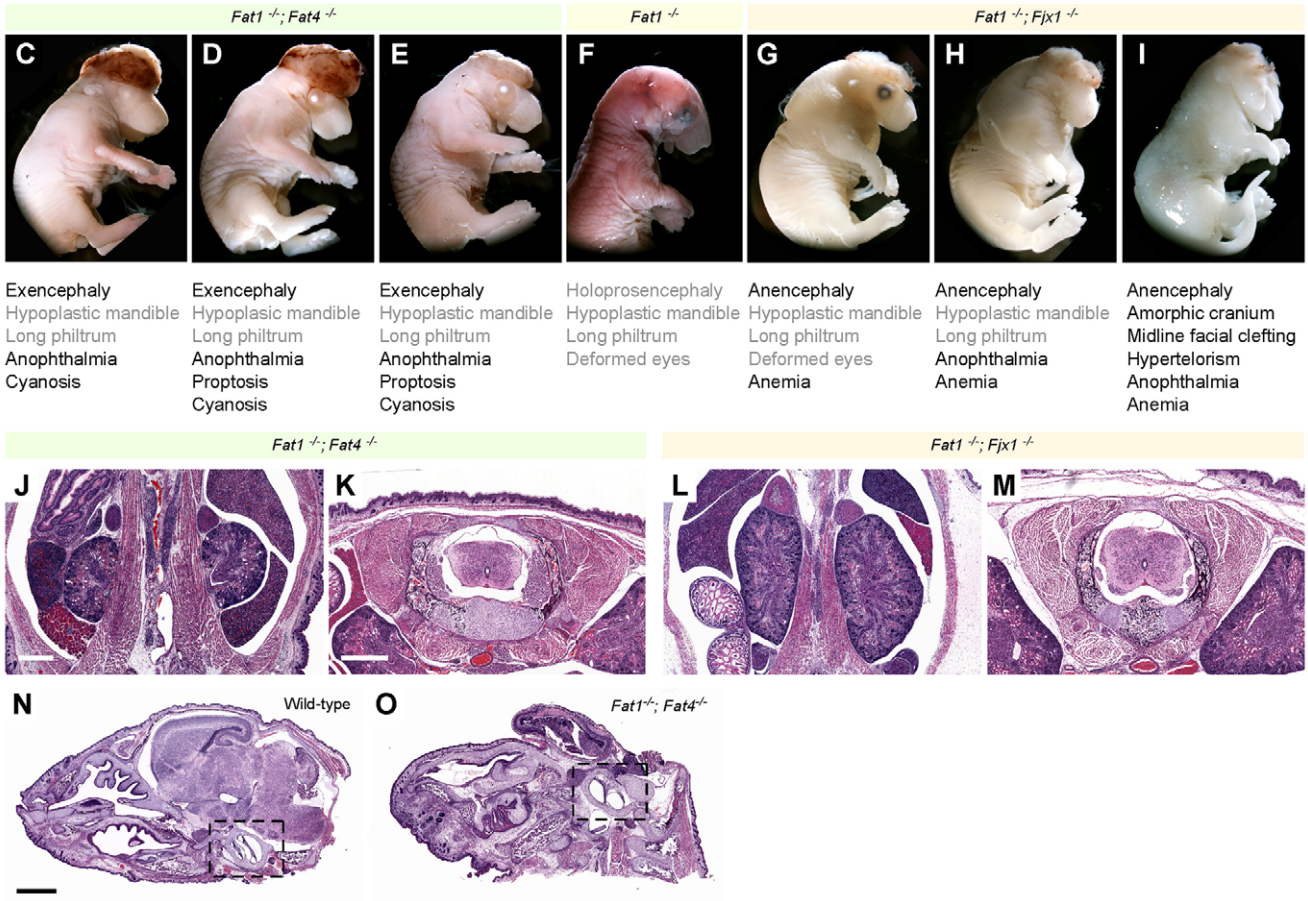

Fig. 4. *Fat1* synergistically interacts with *Fat4* and *Fjx1* in the cranial neural tube. (**A**,**B**) The number of double mutants with cranial neural tube defects. E18.5 mouse embryos were obtained from *Fat1*$^{-/+}$;*Fat4*$^{-/+}$ (A) or *Fat1*$^{-/+}$;*Fjx1*$^{-/+}$ (B) intercrosses. (**C-I**) Appearance of *Fat1*$^{-/-}$;*Fat4*$^{-/-}$ (C-E), *Fat1*$^{-/-}$ (F) or *Fat1*$^{-/-}$;*Fjx1*$^{-/-}$ (G-I) E18.5 embryos. (**J**,**L**) H&E-stained longitudinal sections of E18.5 *Fat1*$^{-/-}$;*Fat4*$^{-/-}$ (J) and *Fat1*$^{-/-}$;*Fjx1*$^{-/-}$ (L) kidneys. (**K**,**M**) H&E-stained transverse sections of E18.5 *Fat1*$^{-/-}$;*Fat4*$^{-/-}$ (K) and *Fat1*$^{-/-}$;*Fjx1*$^{-/-}$ (M) lumbar neural tube and vertebra. (**N**,**O**) H&E-stained longitudinal sections through wild-type (N) and *Fat1*$^{-/-}$;*Fat4*$^{-/-}$ (O) E18.5 heads. Ears are boxed (black dashed lines). Scale bars: 500 μm.

Interactions between Fat3 and Fat4 in kidney, cochlea and vertebrae morphogenesis

Based on our evidence for functional redundancy between *Fat1* and *Fat4*, we asked whether *Fat3* also shares functions with *Fat4*. *Fat3*$^{-/-}$ kidneys are normal, with no significant change in the luminal space of renal tubules (P=0.31; Fig. 5A,B,N). *Fat3*$^{-/-}$;*Fat4*$^{-/-}$ mutants are viable at birth with no external anomalies in craniofacial structure (supplementary material Table S4; data not shown). Surprisingly, cystic defects in *Fat4*$^{-/-}$ kidneys are suppressed upon loss of *Fat3* (P=2.93×10^{-2}; Fig. 5C,D,N), suggesting that Fat3 and Fat4 serve antagonistic functions in controlling renal tubular elongation.

To determine whether Fat3 and Fat4 act antagonistically in other contexts, we examined cochlear development in *Fat3*$^{-/-}$ and *Fat3*$^{-/-}$;*Fat4*$^{-/-}$ mutants. *Fat3*$^{-/-}$ mutants do not display defects in cochlear lengthening (P=0.68; Fig. 5I,J,O). *Fat4*$^{-/-}$ cochlear length is not altered upon loss of *Fat3* (P=0.44; Fig. 5K,L,O). However, in contrast to the gain of subsets of OHC4s in *Fat4*$^{-/-}$ mutants, *Fat3*$^{-/-}$ cochleae exhibited discontinuous loss of OHC3s, with patches of three to ten missing cells, predominantly in the basal turn (P=3.84×10^{-4}; Fig. 5M,Q). Despite these apparently opposing functions, even more OHC3s emerged in the mid-apical region of *Fat3*$^{-/-}$;*Fat4*$^{-/-}$ than *Fat4*$^{-/-}$ cochlea (P=1.38×10^{-2}; Fig. 5Q).

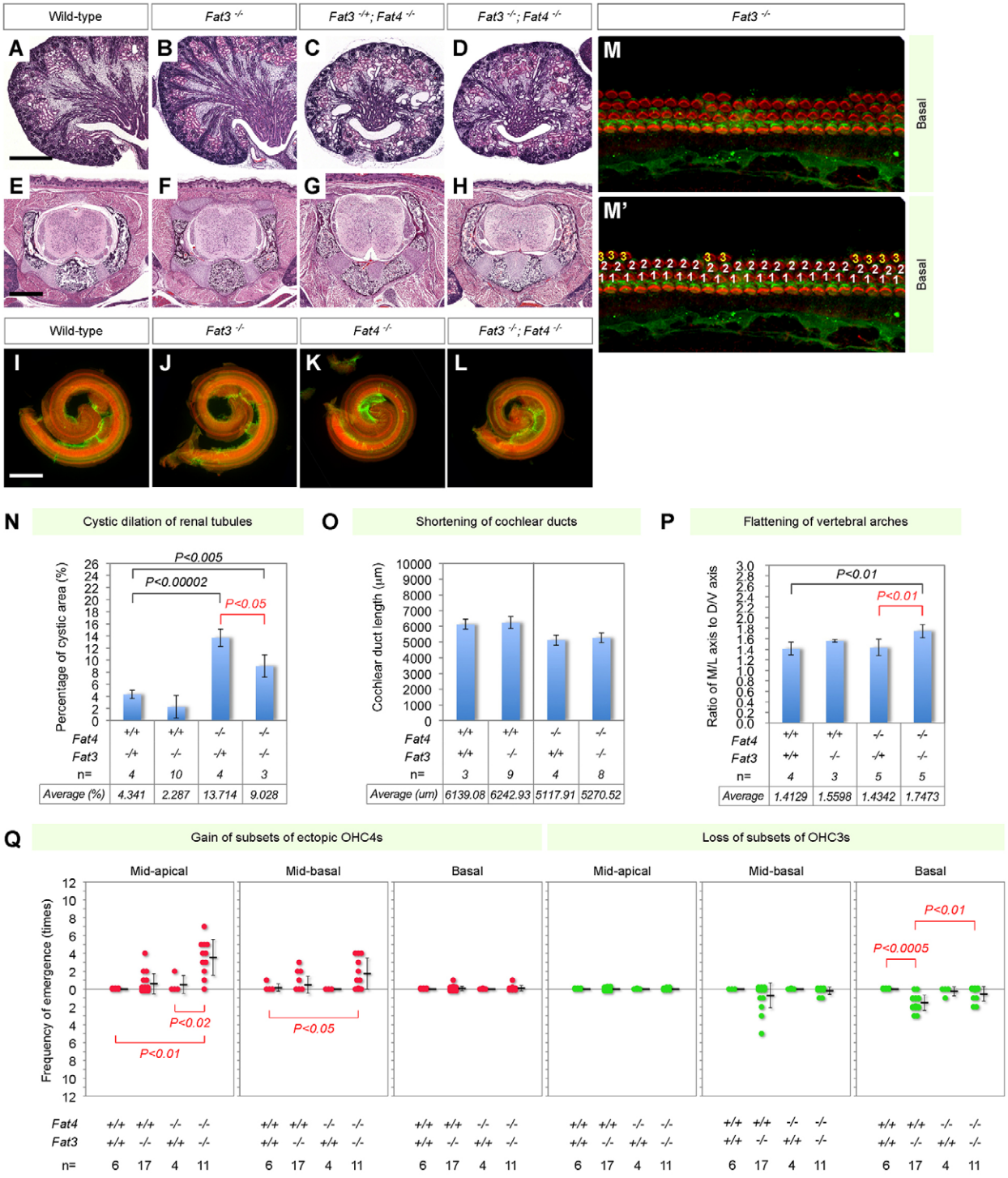

Fig. 5. *Fat3* synergizes with *Fat4* in caudal vertebra, but antagonizes *Fat4* in kidney and cochlea. (**A-D**) H&E-stained longitudinal sections of P0 wild-type (A), *Fat3*$^{-/-}$ (B), *Fat3*$^{-/+}$;*Fat4*$^{-/-}$ (C) and *Fat3*$^{-/-}$;*Fat4*$^{-/-}$ (D) mouse kidney. (**E-H**) H&E-stained transverse sections of P0 wild-type (E), *Fat3*$^{-/-}$ (F), *Fat3*$^{-/+}$;*Fat4*$^{-/-}$ (G) and *Fat3*$^{-/-}$;*Fat4*$^{-/-}$ (H) lumbar vertebra. (**I-L**) Phalloidin-stained cochlear epithelia of P0 wild-type (I), *Fat3*$^{-/-}$ (J), *Fat4*$^{-/-}$ (K) and *Fat3*$^{-/-}$;*Fat4*$^{-/-}$ (L) inner ear. (**M**,**M'**) Immunofluorescence on *Fat3*$^{-/-}$ cochlear sensory epithelium as in Fig. 1G-L'. (**N-P**) Morphometric analyses of renal tubular dilation (N), cochlear shortening (O) and vertebral arch broadening (P). Statistics performed as in Fig. 2P-R. (**Q**) Frequency plots of gain or loss of OHC patches in the OOC. Phenotypic severities defined and presented as in Fig. 2S. Scale bars: 500 μm.

Moreover, fewer OHC3s were lost from the basal turn of *Fat3*$^{-/-}$;*Fat4*$^{-/-}$ than *Fat3*$^{-/-}$ cochleae (P=6.22×10^{-3}; Fig. 5Q). Thus, *Fat3* and *Fat4* exhibit complex interactions during hair cell patterning.

Fat3 and *Fat4* are strongly expressed in both the neural tube and the intervertebral discs during development (Rock et al., 2005). Although morphogenetic anomalies are not evident in the spinal cord or vertebrae of *Fat3*$^{-/-}$ newborns (ML/DV ratio of lumbar

vertebra, P=0.10; Fig. 5E,F,P), incomplete fusion of vertebral arches of *Fat4*$^{-/-}$ mutants increased in severity upon loss of *Fat3* (P=8.68×10^{-3}; Fig. 5G,H,P). Indeed, *Fat3*$^{-/-}$;*Fat4*$^{-/-}$ mutants exhibited severely flattened vertebral arches (Fig. 5H). Thus, Fat3 and Fat4 cooperate during the fusion of vertebral arches.

Synergy between Fat1 and Fjx1 in cranial neural tube morphogenesis

Having revealed overlapping functions for different Fat family genes, we investigated whether any of these phenotypes involve disruption of the Ft/Ds/Fj signaling module. We focused on *Fjx1*, the sole vertebrate ortholog of *Drosophila fj*. Fjx1 is expressed in developing kidneys, cochleae, intervertebral discs and neural tube (Rock et al., 2005). However, *Fjx1*$^{-/-}$ mutants display no apparent defects in any of these tissues (Fig. 6B,F,J,P-S). Similarly, most *Fat4* loss-of-function phenotypes are unaffected by loss of *Fjx1*, with no change in cochlear length (P=0.94; Fig. 6G,H,Q), OHC4 frequency (P=0.45; Fig. 6M,N,O,S) or mediolateral length of lumbar vertebrae (P=0.96; Fig. 6K,L,R) in *Fat4*$^{-/-}$;*Fjx1*$^{-/-}$ mutants as compared with *Fat4*$^{-/-}$ mutants. Loss of *Fjx1* occasionally exacerbates cystic defects in *Fat4*$^{-/-}$ kidneys associated with the development of duplex kidneys and ureteral duplication in a background of [(129P2/Ola × FVB/N)F1 × C57BL/6]F2 (Saburi et al., 2008), but not in the 129S3 background used in this study (P=0.62; Fig. 6C,D,P). *Fat1*$^{-/-}$;*Fjx1*$^{-/-}$ kidneys appear normal at birth, as do *Fat1*$^{-/-}$ kidneys (Fig. 4L).

Although loss of *Fjx1* does not strongly enhance most Fat family phenotypes in a 129S3 background, there are strong genetic interactions in the neural tube. *Fat4*$^{-/-}$;*Fjx1*$^{-/-}$ mutants are born with no anomalies in the cranial neural tube (supplementary material Table S5). Strikingly, however, half of *Fat1*$^{-/-}$;*Fjx1*$^{-/-}$ E18.5 embryos exhibit anencephaly, a severe form of exencephaly accompanied by degeneration of cerebral tissue (Fig. 4B,G-I and supplementary material Tables S6 and S8). Anencephalic double mutants also display severe anemia, indicating impaired hematopoiesis (Fig. 4G,H,I). Moreover, double-mutant embryos occasionally exhibit an amorphous cranium, with a widened frontonasal prominence and midline facial clefting (Fig. 4I). Neither *Fat1*$^{-/-}$ nor *Fjx1*$^{-/-}$ single-mutant siblings showed craniofacial abnormalities on the 129S3 background (Fig. 4B,F and supplementary material Table S6). Even in anencephalic *Fat1*$^{-/-}$;*Fjx1*$^{-/-}$ embryos, no abnormalities are observed in kidneys, spinal cord or lumbar vertebrae (Fig. 4L,M).

Antagonism between Atn1 and Fat4 in caudal vertebra morphogenesis

Drosophila Ft regulates planar polarity through interactions with Atrophin (Fanto et al., 2003). We investigated whether vertebrate Fat4 also interacts with atrophins to control tissue morphogenesis. We first tested whether *Fat4* interacts with *Atn1* in kidney development. Whereas *Atn1*$^{-/-}$ homozygotes have normal kidneys (Fig. 7A,B,N and supplementary material Fig. S6C), *Atn1*$^{-/-}$;*Fat4*$^{-/-}$ kidneys frequently fail to form medulla (supplementary material Fig. S6A,B) and lack loops of Henle and medullary collecting ducts (supplementary material Fig. S6D,E). Because tubular segments were poorly formed in *Atn1*$^{-/-}$;*Fat4*$^{-/-}$ kidneys, we were unable to determine if loss of *Atn1* affects the cystic defects of *Fat4*$^{-/-}$ kidneys. However, cystic dilations were not significantly modified in *Fat4*$^{-/-}$ kidneys upon loss of one copy of *Atn1* (P=0.83; Fig. 7C,D,N). Thus, although kidney organogenesis can be severely impaired in *Atn1*$^{-/-}$;*Fat4*$^{-/-}$ kidneys, we were unable to determine whether genetic interactions with *Atn1* can enhance the cystic defects in *Fat4*$^{-/-}$ kidneys.

We examined whether *Fat4* requires *Atn1* to control cochlear elongation and OHC patterning. The cochlear length is comparable in wild type and *Atn1*$^{-/-}$ mutants (P=0.88; Fig. 7E,F,O). Simultaneous loss of *Atn1* and *Fat4* does not modify cochlear length in *Fat4*$^{-/-}$ mutants (P=0.70; Fig. 7G,H,O). Similarly, neither additional rows nor misorientations of sensory hair cells are observed in *Atn1*$^{-/-}$ cochleae (Fig. 7M,Q). *Atn1*$^{-/-}$ mutants exhibit occasional discontinuous loss of OHC3s in the basal turn of cochleae, as in *Fat3*$^{-/-}$ mutants, although the *Atn1*$^{-/-}$ defects are not statistically significant (P=0.13; Fig. 7M,Q). Loss of OHC3s was not observed in *Fat4*$^{-/-}$ cochleae (Fig. 2S, Fig. 3S, Fig. 5Q, Fig. 6S, Fig. 7Q, Fig. 8S). Loss of OHC3s in *Atn1*$^{-/-}$ cochleae decreased in frequency upon loss of *Fat4*, but this was statistically insignificant compared with siblings (P=0.10; Fig. 7Q). Occasional OHC3 loss occurred even in wild-type siblings (Fig. 7Q). As 129S3 wild-type cochleae never display loss of OHC3s (supplementary material Fig. S3D), this is likely to be due to a strain-specific variant unlinked to *Atn1*.

Loss of *Atn1* does not dramatically disrupt morphogenesis of the neural tube or vertebra (Fig. 7I,J and supplementary material Tables S7, S8), as shown by measuring the ML/DV ratio of lumbar vertebra (P=0.06; Fig. 7P). Moreover, lumbar spinal cords are not significantly broadened in *Atn1*$^{-/-}$;*Fat4*$^{-/-}$ mutants (Fig. 7L; data not shown). By contrast, improper fusion of vertebral arches is slightly suppressed in *Fat4*$^{-/-}$ mutants upon loss of *Atn1* (P=2.26×10^{-2}; Fig. 7K,L,P), suggesting that *Atn1* functions antagonistically to *Fat4* during vertebral arch fusion.

Synergy between Atn2l and Fat4 in kidney and cochlea morphogenesis

We wondered whether a second *atro*-like gene, *Atn2l*, which is most similar to *Drosophila atro*, functions in *Fat4* activity. Homozygous *Atn2 om* mutation leads to embryonic lethality between E9.5 and E11.5 associated with cardiac failure (Zoltewicz et al., 2004), precluding determination of whether renal tubular morphogenesis is perturbed in *Atn2*$^{om/om}$ kidneys. Whereas kidneys develop normally in *Atn2*$^{om/+}$ heterozygotes (Fig. 8A,B,P), removal of one copy of *Atn2l* enhances cystic defects in *Fat4*$^{-/-}$ kidneys (P=1.37×10^{-2}; Fig. 8C,D,P). This enhancement is similar to the exacerbation of cystic defects observed in *Fat4*$^{-/-}$;*Vangl2*$^{Lp/+}$ kidneys, suggesting that *Atn2l* and *Fat4* function in planar polarity patterning in the kidney.

Whereas *Atn2*$^{om/+}$ cochleae show no defects in hair cell organization (Fig. 8S), *Atn2*$^{om/+}$;*Fat4*$^{-/-}$ mutants occasionally develop a fourth row of OHCs, predominantly in the mid-apical region (Fig. 8S). This effect is similar to what occurs in *Fat4*$^{-/-}$;*Vangl2*$^{Lp/+}$ and *Fat1*$^{-/+}$;*Fat4*$^{-/-}$ cochleae, but opposite to the loss of OHC3s seen in *Atn1*$^{-/-}$ and *Fat3*$^{-/-}$ cochleae. Loss of OHC3s was never observed in *Fat4*$^{-/-}$ cochleae (Fig. 2S, Fig. 3S, Fig. 6S, Fig. 8S). *Atn2l* haploinsufficiency does not affect cochlear lengthening (Fig. 8E,F,Q) and *Fat4*$^{-/-}$ cochlear length is not significantly modified upon removal of one copy of *Atn2l* (P=0.83; Fig. 8G,H,Q).

We tested whether spinal cord or vertebral anomalies in *Fat4*$^{-/-}$ mutants are enhanced by loss of one copy of *Atn2l*. *Atn2*$^{om/+}$ heterozygotes exhibit no malformations in the spinal cord or vertebrae (Fig. 8I,J,R). Moreover, neither the widening of spinal cord nor improper fusion of vertebral arches is modified in *Atn2*$^{om/+}$;*Fat4*$^{-/-}$ mutants as compared with *Fat4*$^{-/-}$ siblings (P=0.25; Fig. 8K,L,R).

Atn2 om mutants exhibit complete failure in cranial neural tube closure, particularly in the forebrain (Zoltewicz et al., 2004). However, no *Atn2l* haploinsufficiency is observed in cranial neural tube formation. Although *Fat1*$^{-/-}$;*Fat4*$^{-/-}$ mutants display

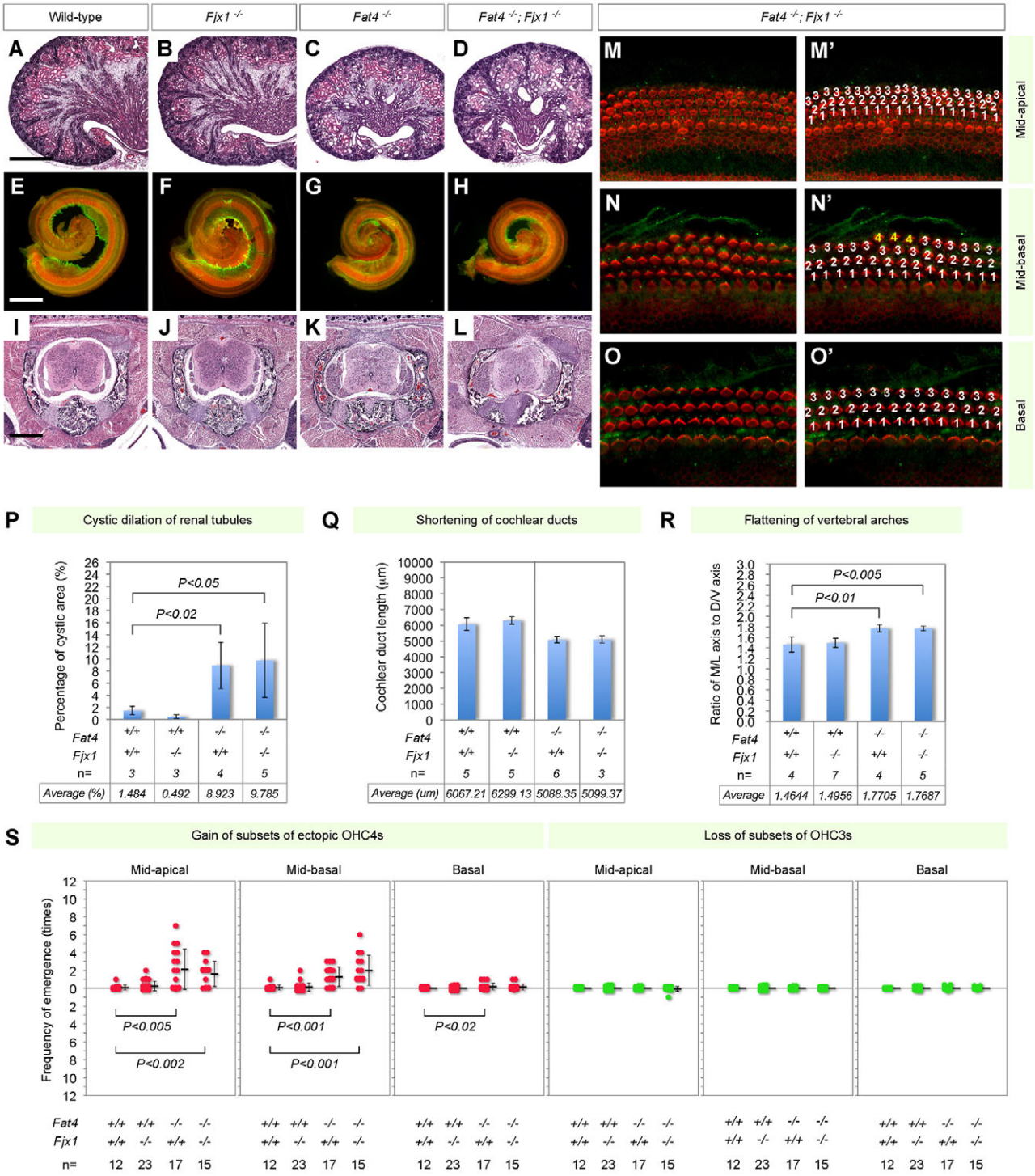

Fig. 6. *Fjx1* does not interact with *Fat4* in kidney, cochlea or caudal vertebra. (**A-D**) H&E-stained longitudinal sections of P0 wild-type (A), *Fjx1*$^{-/-}$ (B), *Fat4*$^{-/-}$ (C) and *Fat4*$^{-/-}$;*Fjx1*$^{-/-}$ (D) mouse kidney. (**E-H**) Phalloidin-stained cochlear epithelia of P0 wild-type (E), *Fjx1*$^{-/-}$ (F), *Fat4*$^{-/-}$ (G) and *Fat4*$^{-/-}$;*Fjx1*$^{-/-}$ (H) inner ear. (**I-L**) H&E-stained transverse sections of P0 wild-type (I), *Fjx1*$^{-/-}$ (J), *Fat4*$^{-/-}$ (K) and *Fat4*$^{-/-}$;*Fjx1*$^{-/-}$ (L) lumbar vertebra. (**M-O′**) Immunofluorescence on *Fat4*$^{-/-}$;*Fjx1*$^{-/-}$ cochlear sensory epithelium as in Fig. 1G-L′. (**P-R**) Morphometric analyses of renal tubular dilation (P), cochlear shortening (Q) and vertebral arch broadening (R). Statistics performed as in Fig. 2P-R. (**S**) Frequency plots of gain or loss of OHC patches in the OOC. Phenotypic severities defined and presented as in Fig. 2S. Scale bars: 500 μm.

exencephaly, reminiscent of the fully penetrant neural tube defects in *Atn2 om* mutants, *Atn2*$^{om/+}$;*Fat4*$^{-/-}$ mutants are born at the predicted Mendelian ratio with no detectable abnormalities in the cranial neural tube (supplementary material Table S9).

DISCUSSION

Fat cadherins regulate a wide variety of developmental events in flies, including planar polarity, tissue growth and organ shape. Previously, we showed that *Fat4* plays a key role in planar

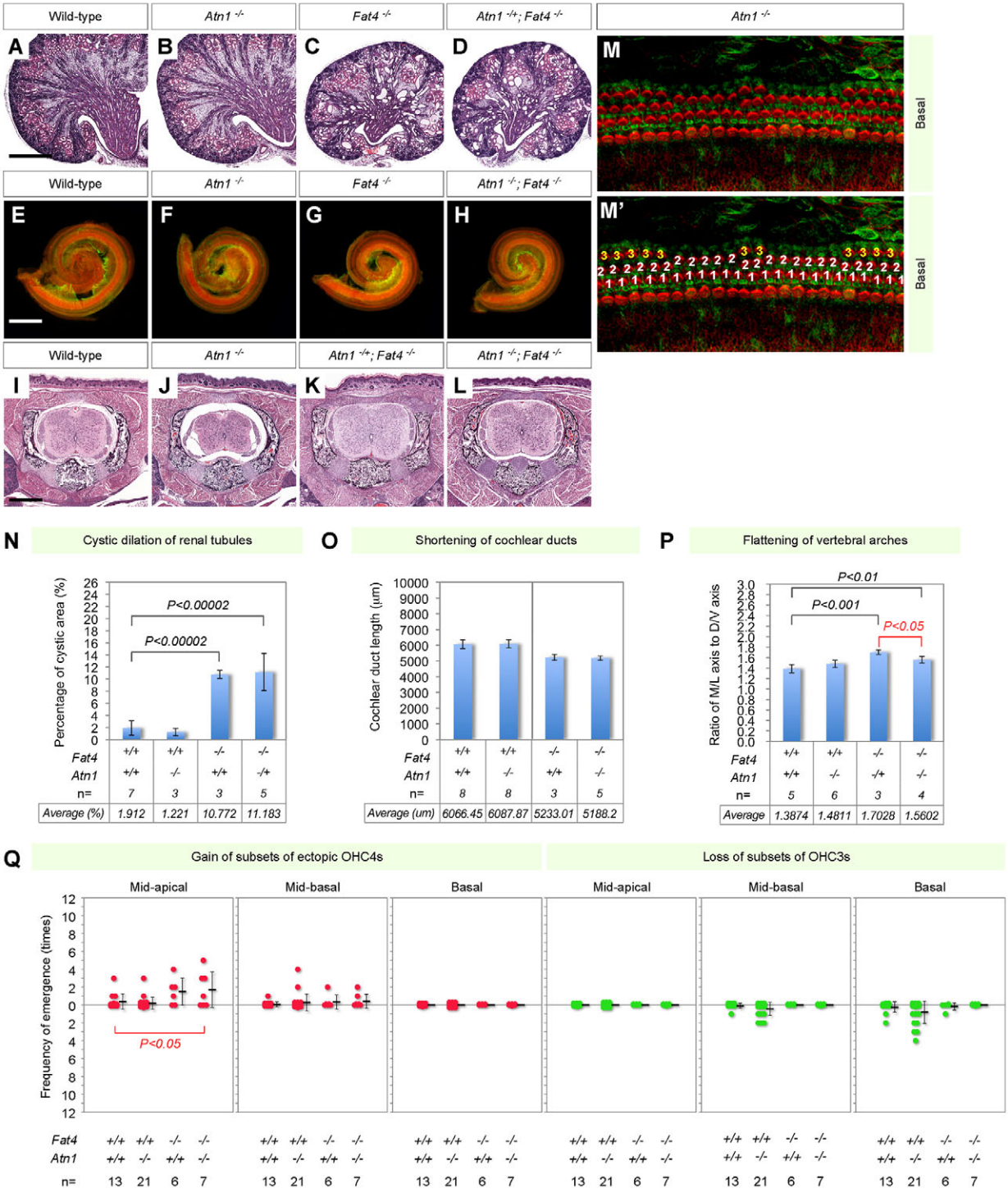

Fig. 7. *Atn1* antagonizes *Fat4* in caudal vertebra. (**A-D**) H&E-stained longitudinal sections of a P0 wild-type (A), *Atn1*$^{-/-}$ (B), *Fat4*$^{-/-}$ (C) and *Atn1*$^{-/+}$;*Fat4*$^{-/-}$ (D) mouse kidney. (**E-H**) Phalloidin-stained cochlear epithelia of P0 wild-type (E), *Atn1*$^{-/-}$ (F), *Fat4*$^{-/-}$ (G) and *Atn1*$^{-/-}$;*Fat4*$^{-/-}$ (H) inner ear. (**I-L**) H&E-stained transverse sections of P0 wild-type (I), *Atn1*$^{-/-}$ (J), *Atn1*$^{-/+}$;*Fat4*$^{-/-}$ (K) and *Atn1*$^{-/-}$;*Fat4*$^{-/-}$ (L) lumbar vertebra. (**M**,**M'**) Immunofluorescence on *Atn1*$^{-/-}$ cochlear sensory epithelium as in Fig. 1G-L'. (**N-P**) Morphometric analyses of renal tubular dilation (N), cochlear shortening (O) and vertebral arch broadening (P). Statistics performed as in Fig. 2P-R. (**Q**) Frequency plots of gain or loss of OHC patches in the OOC. Phenotypic severities defined and presented as in Fig. 2S. Scale bars: 500 μm.

polarity in mammals, as *ft* does in flies. However, it has not been clear whether other Fat family members play similar roles and whether other components of the Fat-planar polarity pathway are also conserved from flies to human. Here, we report that mouse Fat1 and Fat3 cooperate with Fat4 in a number of developmental contexts, including kidney, cochlea, cranial neural tube and caudal vertebra. In addition, we provide genetic evidence that the roles for Fat4 in renal tubular elongation,

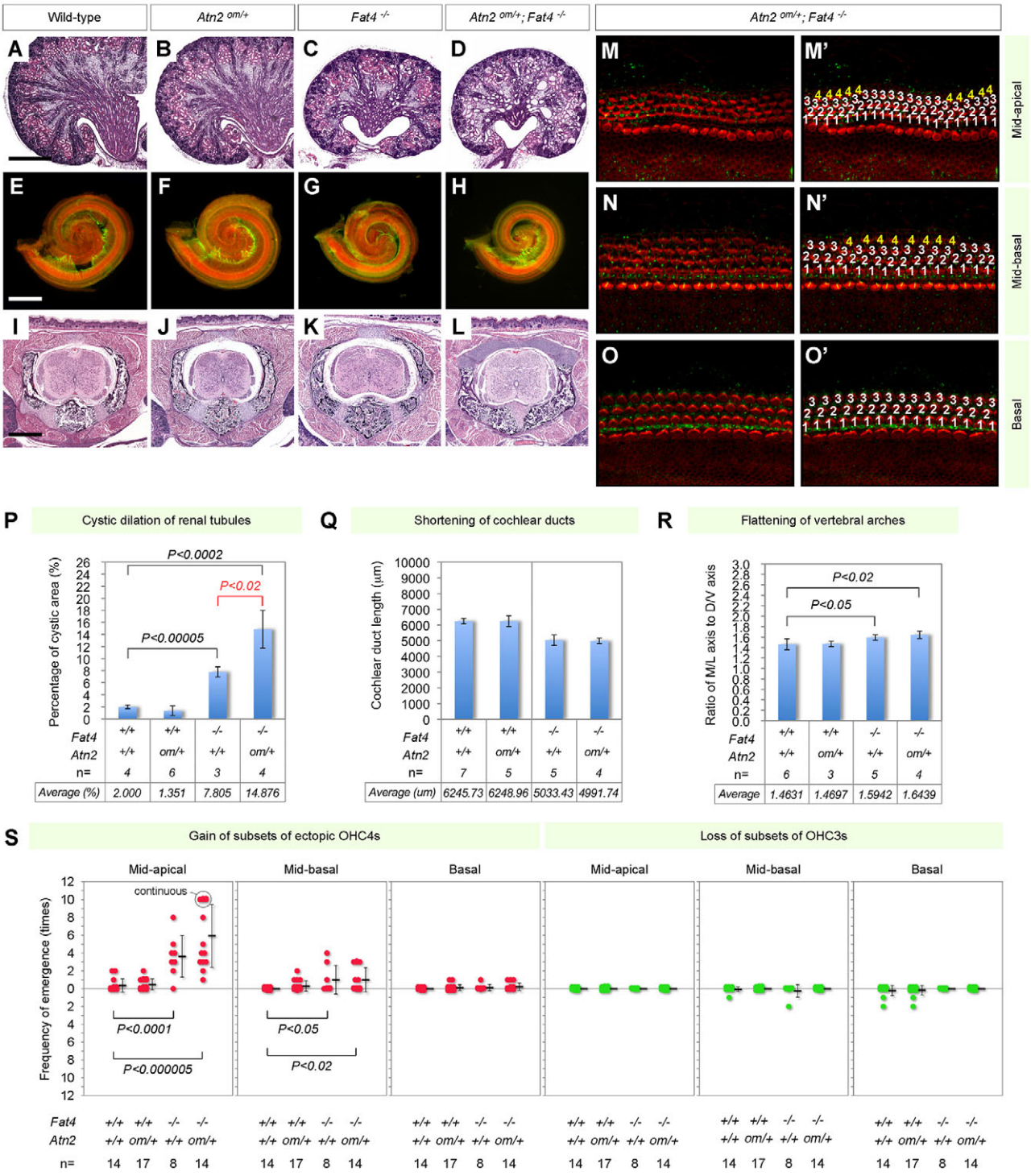

Fig. 8. *Atn2l* cooperates with *Fat4* in kidney and cochlea. (**A-D**) H&E-stained longitudinal sections of P0 wild-type (A), *Atn2l*$^{om/+}$ (B), *Fat4*$^{-/-}$ (C) and *Atn2l*$^{om/+}$;*Fat4*$^{-/-}$ (D) mouse kidney. (**E-H**) Phalloidin-stained cochlear epithelia of P0 wild-type (E), *Atn2l*$^{om/+}$ (F), *Fat4*$^{-/-}$ (G) and *Atn2l*$^{om/+}$;*Fat4*$^{-/-}$ (H) inner ears. (**I-L**) H&E-stained transverse sections of P0 wild-type (I), *Atn2l*$^{om/+}$ (J), *Fat4*$^{-/-}$ (K) and *Atn2l*$^{om/+}$;*Fat4*$^{-/-}$ (L) lumbar vertebra. (**M-O′**) Immunofluorescence on *Atn2l*$^{om/+}$;*Fat4*$^{-/-}$ cochlear sensory epithelium as in Fig. 1G-L′. (**P-R**) Morphometric analyses of renal tubular dilation (P), cochlear shortening (Q) and vertebral arch broadening (R). Statistics performed as in Fig. 2P-R. (**S**) Frequency plots of gain or loss of OHC patches in the OOC. Phenotypic severities were defined and presented as in Fig. 2S. Scale bars: 500 μm.

vertebral arch fusion and OHC patterning are modified by vertebrate atrophins. Together with evidence that a *Vangl2 Lp* mutation enhances multiple *Fat4*$^{-/-}$ phenotypes, these findings suggest that *Fat4* acts through a conserved pathway to control planar polarity. Further studies will be needed to uncover the biochemical and molecular bases of the genetic interactions among Fat cadherins and atrophins in regulating tissue organization.

We found that proper elongation of renal tubules in the kidneys involves both *Fat1* and *Fat4*, raising the question of how each *ft*-like gene mediates its effects. One intriguing possibility is that Fat cadherins act through the Hippo signaling pathway, as attenuation of Hippo signaling contributes to renal cyst formation in *fat1* morphant zebrafish (Skouloudaki et al., 2009). A role for Hippo signaling in renal tubular morphogenesis is also supported by recent genetic studies in mice and humans (Happe et al., 2011; Hossain et al., 2007; Makita et al., 2008).

Fat1 physically interacts with atrophins (Hou and Sibinga, 2009). We showed here that removal of one copy of *Atn2l*, but not *Atn1*, makes renal tubular elongation more sensitive to loss of *Fat4*, does loss of one copy of *Fat1*. These observations suggest that Fat1 compensates for Fat4 through interactions with Atn2l. Because it remains to be determined whether Atn2l binds to Fat4, synergy between *Fat1* and *Fat4* in this context might be mediated by sharing of the effector, Atn2l, and/or by parallel action of Fat1-Atn2l to Fat4 signaling (supplementary material Fig. S7).

Additional complexities in Fat functions are revealed in cochleae, where both synergistic and antagonistic effects were observed. *Fat1* and *Fat4* again act synergistically here, as cochlear shortening was exacerbated and the emergence of ectopic OHC4s was enhanced in the basal turn of $Fat1^{-/+};Fat4^{-/-}$ cochleae. By contrast, $Fat3^{-/-}$ cochleae display discontinuous loss of OHC3s near the base and loss of OHC3s can be suppressed by loss of *Fat4*. Thus, *Fat4* interacts cooperatively with *Fat1* to stimulate cochlear extension and limit OHC row number, but antagonistically with *Fat3* in OHC patterning (supplementary material Fig. S7).

The cochlear phenotype in $Fat4^{-/-}$ mutants is consistent with disrupted planar polarity signaling. Planar polarity is necessary for CE movements associated with cochlear elongation, and mutations in core PCP genes result in expansion in OHC row number in the apex (Etheridge et al., 2008; Montcouquiol et al., 2003; Yu et al., 2010). The core PCP mutants also exhibit disorganization of hair cells near the base, namely ectopic hair cells beyond the OHC3s (Wang, Y. et al., 2006), as seen in the $Fat1^{-/+};Fat4^{-/-}$ cochleae. The fact that cochlear elongation is impaired in $Fat4^{-/-}$ mutants and that $Fat4^{-/-}$ cochleae become shorter still in the $Vangl2^{Lp/+}$ background suggest that both *Fat4* and *Vangl2* control planar polarity in cochlea. Emergence of ectopic OHC4s was also exacerbated in the mid-apical turn of $Fat4^{-/-};Vangl2^{Lp/+}$ cochleae. As in flies, whether Fat4 and core PCP components act in parallel or together remains unknown. Intriguingly, defects in both cochlea elongation and OHC patterning in $Fat4^{-/-}$ mutants are exacerbated upon loss of one copy of *Fat1*, suggesting that *Fat1* might influence planar polarity in cochlea. As in the kidney, impaired OHC patterning in $Fat4^{-/-}$ cochleae, but not cochlear shortening, increased in severity upon removal of one copy of *Atn2l*, suggesting that synergy between *Fat1* and *Fat4* in the OOC might be mediated by Atn2l as described above (supplementary material Fig. S7).

Analysis of vertebral development revealed additional redundancies amongst Fat family cadherins. $Fat4^{-/-}$ mutants display malformed vertebral arches caused by failure in fusion at the dorsal midline. A similar phenotype was reported in $Dchs1^{-/-}$ mutants (Mao et al., 2011), suggesting that Dchs1 is a Fat4 ligand (Ishiuchi et al., 2009; Mao et al., 2011). The vertebral phenotype in $Fat4^{-/-}$ mutants increased in severity upon loss of *Fat3*, suggesting that *Fat3* and *Fat4* act together in intervertebral discs to direct proper fusion of vertebral arches (supplementary material Fig. S7). Although little is known about the cellular events that underlie this process, incomplete fusion might be a PCP phenotype, as $Dvl1^{-/-};Dvl2^{-/-}$ mutants also display wide vertebral columns accompanied by classic PCP phenotypes such as looped tails, opened neural tube and abnormal cochlear extension (Hamblet et al., 2002). In support of this idea, impaired fusion of vertebral arches in $Fat4^{-/-}$ mutants was occasionally exacerbated by $Vangl2^{Lp/+}$ heterozygosity.

The remarkable breadth of Fat activities is highlighted in the nervous system, where once again Fat family members have both overlapping and distinct functions. *Fat1* seems to be a key player in the cranial neural tube, whereas *Fat4* acts more caudally. Some of these functions might reflect functional redundancy, as $Fat1^{-/-};Fat4^{-/-}$ mutants suffer from an increased incidence of exencephaly compared with $Fat1^{-/-}$ or $Fat4^{-/-}$ mutants. However, *Fat1* and *Fat4* appear to have independent functions during neural tube morphogenesis. For instance, *Fat1* shows unique synergy with *Fjx1*, as $Fat1^{-/-};Fjx1^{-/-}$ mutants exhibit anencephaly, whereas $Fat4^{-/-};Fjx1^{-/-}$ mutants display no detectable anomalies in the cranial neural tube. *Drosophila* Fj is a kinase that phosphorylates the extracellular cadherin domains of both Ft and Ds, modifying their ability to bind to each other (Brittle et al., 2010; Ishikawa et al., 2008; Simon et al., 2010). Thus, Fjx1 might regulate Fat and Dachsous cadherins in vertebrates, altering their physical interactions. Consistent with this model, loss of *Fjx1* enhances $Fat3^{-/+}$ but not $Fat3^{-/-}$ phenotypes in retina (Deans et al., 2011). Taken together, Fat cadherins may function in parallel, downstream of Fjx1, to regulate cranial neural tube development. Because loss of *Fat1* may induce *Fjx1* expression, as *ft* or *Fat4* mutation does in flies or mice (Fanto et al., 2003; Saburi et al., 2008), simultaneous loss of *Fat1* and *Fjx1* might also disrupt a feedback loop for other Fat and Dachsous cadherins to compensate for *Fat1* (supplementary material Fig. S7).

It remains to be determined whether the exencephaly and anencephaly in $Fat1^{-/-};Fat4^{-/-}$ and $Fat1^{-/-};Fjx1^{-/-}$ mutants are due to abnormal planar polarity signaling. However, synergies similar to those we found for Fat family genes are also observed in the cranial neural tube for core PCP genes (Fischer et al., 2007). Loss of *Fz3* leads to failure of cephalic neural tube closure at low penetrance depending on genetic background (Wang et al., 2002), whereas $Fz6^{-/-}$ mutants do not have specific deformities in the neural tube. However, simultaneous loss of *Fz3* and *Fz6* causes craniorachischisis with nearly complete penetrance (Wang, Y. et al., 2006), and *Fz3* heterozygosity is sufficient to induce severe anencephaly in $Fz6^{-/-}$ mutants, although with reduced penetrance (Stuebner et al., 2010). Alternatively, *Fat4* could play a role in the caudal neural tube via the Hippo signaling pathway. Indeed, a recent study revealed a role for *Fat4* in the restriction of cell numbers in the neuronal progenitor pools in the chick neural tube, via the Hippo mediator YAP (Van Hateren et al., 2011), raising the possibility that the broadened spinal cords in the $Fat4^{-/-}$ mouse mutants might be caused by aberrant expansion of neural progenitors.

Conclusions

Fat cadherins comprise a diverse family of proteins with substantially different intracellular domains, and we have shown here that some function redundantly to pattern tissues, whereas others function antagonistically. Moreover, Fat family members exhibit tissue-specific interactions, such as *Fat1* and *Fat4* in kidney, cochlea, cranial neural tube and *Fat3* and *Fat4* in vertebra. Although several Fat loss-of-function phenotypes in mice reflect altered planar polarity signaling, such as cystic kidneys and shortened cochleae (Mao et al., 2011; Saburi et al., 2008), other phenotypes may not be due to defective planar polarity and might

instead reflect altered growth regulation. Consistent with this model, only a subset of *Fat4*$^{-/-}$ phenotypes is enhanced by disrupted *Vangl2* activity. Our data also suggest that atrophins might function with Fat cadherins in vertebrates, as in flies, to regulate planar polarity. Finally, we have seen strong inbred genetic background effects in Fat loss-of-function phenotypes, not only in the cranial neural tube, which generally shows a clear strain dependency of defects (Banting et al., 2005; Choi and Klingensmith, 2009; Colmenares et al., 2002; Ikeda et al., 1999; Kaneko et al., 2007; Kooistra et al., 2012; Sah et al., 1995; Sang et al., 2011; Stottmann et al., 2006; Wright et al., 2007), but also in other tissues. These as yet unidentified modifiers might impact the distinct phenotypic readouts caused by loss of Fat, such as defective Fat-planar polarity signaling versus Fat-Hippo signaling. Although these complexities introduce new challenges, our findings emphasize the wide-ranging impact that Fat cadherins have on animal development.

Acknowledgements
We thank Michael Dean for insightful comments and discussions.

Funding
Supported by the Canadian Institutes of Health Research [grant FRN-MOP84468 to H.M.]. L.G. is supported by the National Institutes of Health. Deposited in PMC for release after 12 months.

Competing interests statement
The authors declare no competing financial interests.

Supplementary material
Supplementary material available online at
http://dev.biologists.org/lookup/suppl/doi:10.1242/dev.077461/-/DC1

References

Axelrod, J. D. (2009). Progress and challenges in understanding planar cell polarity signaling. *Semin. Cell Dev. Biol.* **20**, 964-971.
Banting, G. S., Barak, O., Ames, T. M., Burnham, A. C., Kardel, M. D., Cooch, N. S., Davidson, C. E., Godbout, R., McDermid, H. E. and Shiekhattar, R. (2005). CECR2, a protein involved in neurulation, forms a novel chromatin remodeling complex with SNF2L. *Hum. Mol. Genet.* **14**, 513-524.
Barlow, J. L., Drynan, L. F., Hewett, D. R., Holmes, L. R., Lorenzo-Abalde, S., Lane, A. L., Jolin, H. E., Pannell, R., Middleton, A. J., Wong, S. H. et al. (2010). A p53-dependent mechanism underlies macrocytic anemia in a mouse model of human 5q- syndrome. *Nat. Med.* **16**, 59-66.
Brittle, A. L., Repiso, A., Casal, J., Lawrence, P. A. and Strutt, D. (2010). Four-jointed modulates growth and planar polarity by reducing the affinity of dachsous for fat. *Curr. Biol.* **20**, 803-810.
Brooker, R., Hozumi, K. and Lewis, J. (2006). Notch ligands with contrasting functions: Jagged1 and Delta1 in the mouse inner ear. *Development* **133**, 1277-1286.
Brunskill, E. W., Lai, H. L., Jamison, D. C., Potter, S. S. and Patterson, L. T. (2011). Microarrays and RNA-Seq identify molecular mechanisms driving the end of nephron production. *BMC Dev. Biol.* **11**, 15-26.
Castillejo-Lopez, C., Arias, W. M. and Baumgartner, S. (2004). The fat-like gene of Drosophila is the true orthologue of vertebrate fat cadherins and is involved in the formation of tubular organs. *J. Biol. Chem.* **279**, 24034-24043.
Choi, M. and Klingensmith, J. (2009). Chordin is a modifier of tbx1 for the craniofacial malformations of 22q11 deletion syndrome phenotypes in mouse. *PLoS Genet.* **5**, e1000395.
Ciani, L., Patel, A., Allen, N. D. and ffrench-Constant, C. (2003). Mice lacking the giant protocadherin mFAT1 exhibit renal slit junction abnormalities and a partially penetrant cyclopia and anophthalmia phenotype. *Mol. Cell. Biol.* **23**, 3575-3582.
Colmenares, C., Heilstedt, H. A., Shaffer, L. G., Schwartz, S., Berk, M., Murray, J. C. and Stavnezer, E. (2002). Loss of the SKI proto-oncogene in individuals affected with 1p36 deletion syndrome is predicted by strain-dependent defects in Ski$^{-/-}$ mice. *Nat. Genet.* **30**, 106-109.
Deans, M. R., Krol, A., Abraira, V. E., Copley, C. O., Tucker, A. F. and Goodrich, L. V. (2011). Control of neuronal morphology by the atypical cadherin Fat3. *Neuron* **71**, 820-832.
Etheridge, S. L., Ray, S., Li, S., Hamblet, N. S., Lijam, N., Tsang, M., Greer, J., Kardos, N., Wang, J., Sussman, D. J. et al. (2008). Murine dishevelled 3 functions in redundant pathways with dishevelled 1 and 2 in normal cardiac outflow tract, cochlea, and neural tube development. *PLoS Genet.* **4**, e1000259.
Fanto, M., Clayton, L., Meredith, J., Hardiman, K., Charroux, B., Kerridge, S. and McNeill, H. (2003). The tumor-suppressor and cell adhesion molecule Fat controls planar polarity via physical interactions with Atrophin, a transcriptional co-repressor. *Development* **130**, 763-774.
Fischer, T., Guimera, J., Wurst, W. and Prakash, N. (2007). Distinct but redundant expression of the Frizzled Wnt receptor genes at signaling centers of the developing mouse brain. *Neuroscience* **147**, 693-711.
Goodrich, L. V. (2008). The plane facts of PCP in the CNS. *Neuron* **60**, 9-16.
Goodrich, L. V. and Strutt, D. (2011). Principles of planar polarity in animal development. *Development* **138**, 1877-1892.
Gray, R. S., Roszko, I. and Solnica-Krezel, L. (2011). Planar cell polarity: coordinating morphogenetic cell behaviors with embryonic polarity. *Dev. Cell* **21**, 120-133.
Guo, N., Hawkins, C. and Nathans, J. (2004). Frizzled6 controls hair patterning in mice. *Proc. Natl. Acad. Sci. USA* **101**, 9277-9281.
Gutzeit, H. O., Eberhardt, W. and Gratwohl, E. (1991). Laminin and basement membrane-associated microfilaments in wild-type and mutant Drosophila ovarian follicles. *J. Cell Sci.* **100**, 781-788.
Hamblet, N. S., Lijam, N., Ruiz-Lozano, P., Wang, J., Yang, Y., Luo, Z., Mei, L., Chien, K. R., Sussman, D. J. and Wynshaw-Boris, A. (2002). Dishevelled 2 is essential for cardiac outflow tract development, somite segmentation and neural tube closure. *Development* **129**, 5827-5838.
Happe, H., van der Wal, A. M., Leonhard, W. N., Kunnen, S. J., Breuning, M. H., de Heer, E. and Peters, D. J. (2011). Altered Hippo signalling in polycystic kidney disease. *J. Pathol.* **224**, 133-142.
Hossain, Z., Ali, S. M., Ko, H. L., Xu, J., Ng, C. P., Guo, K., Qi, Z., Ponniah, S., Hong, W. and Hunziker, W. (2007). Glomerulocystic kidney disease in mice with a targeted inactivation of Wwtr1. *Proc. Natl. Acad. Sci. USA* **104**, 1631-1636.
Hou, R. and Sibinga, N. E. (2009). Atrophin proteins interact with the Fat1 cadherin and regulate migration and orientation in vascular smooth muscle cells. *J. Biol. Chem.* **284**, 6955-6965.
Ikeda, S., Hawes, N. L., Chang, B., Avery, C. S., Smith, R. S. and Nishina, P. M. (1999). Severe ocular abnormalities in C57BL/6 but not in 129/Sv p53-deficient mice. *Invest. Ophthalmol. Vis. Sci.* **40**, 1874-1878.
Ishikawa, H. O., Takeuchi, H., Haltiwanger, R. S. and Irvine, K. D. (2008). Four-jointed is a Golgi kinase that phosphorylates a subset of cadherin domains. *Science* **321**, 401-404.
Ishiuchi, T., Misaki, K., Yonemura, S., Takeichi, M. and Tanoue, T. (2009). Mammalian Fat and Dachsous cadherins regulate apical membrane organization in the embryonic cerebral cortex. *J. Cell Biol.* **185**, 959-967.
Kaneko, K. J., Kohn, M. J., Liu, C. and DePamphilis, M. L. (2007). Transcription factor TEAD2 is involved in neural tube closure. *Genesis* **45**, 577-587.
Kooistra, M. K., Leduc, R. Y., Dawe, C. E., Fairbridge, N. A., Rasmussen, J., Man, J. H., Bujold, M., Juriloff, D., King-Jones, K. and McDermid, H. E. (2012). Strain-specific modifier genes of Cecr2-associated exencephaly in mice: genetic analysis and identification of differentially expressed candidate genes. *Physiol. Genomics* **44**, 35-46.
Lawrence, P. A., Struhl, G. and Casal, J. (2008). Do the protocadherins Fat and Dachsous link up to determine both planar cell polarity and the dimensions of organs? *Nat. Cell Biol.* **10**, 1379-1382.
Makita, R., Uchijima, Y., Nishiyama, K., Amano, T., Chen, Q., Takeuchi, T., Mitani, A., Nagase, T., Yatomi, Y., Aburatani, H. et al. (2008). Multiple renal cysts, urinary concentration defects, and pulmonary emphysematous changes in mice lacking TAZ. *Am. J. Physiol. Renal Physiol.* **294**, F542-F553.
Mao, Y., Mulvaney, J., Zakaria, S., Yu, T., Morgan, K. M., Allen, S., Basson, M. A., Francis-West, P. and Irvine, K. D. (2011). Characterization of a Dchs1 mutant mouse reveals requirements for Dchs1-Fat4 signaling during mammalian development. *Development* **138**, 947-957.
Matakatsu, H. and Blair, S. S. (2004). Interactions between Fat and Dachsous and the regulation of planar cell polarity in the Drosophila wing. *Development* **131**, 3785-3794.
Mitsui, K., Nakajima, D., Ohara, O. and Nakayama, M. (2002). Mammalian fat3: a large protein that contains multiple cadherin and EGF-like motifs. *Biochem. Biophys. Res. Commun.* **290**, 1260-1266.
Moeller, M. J., Soofi, A., Braun, G. S., Li, X., Watzl, C., Kriz, W. and Holzman, L. B. (2004). Protocadherin FAT1 binds Ena/VASP proteins and is necessary for actin dynamics and cell polarization. *EMBO J.* **23**, 3769-3779.
Montcouquiol, M., Rachel, R. A., Lanford, P. J., Copeland, N. G., Jenkins, N. A. and Kelley, M. W. (2003). Identification of Vangl2 and Scrb1 as planar polarity genes in mammals. *Nature* **423**, 173-177.
Montcouquiol, M., Sans, N., Huss, D., Kach, J., Dickman, J. D., Forge, A., Rachel, R. A., Copeland, N. G., Jenkins, N. A., Bogani, D., Murdoch, J., Warchol, M. E., Wenthold, R. J. and Kelley, M. W. (2006). Asymmetric localization of Vangl2 and Fz3 indicate novel mechanisms for planar cell polarity in mammals. *J. Neurosci.* **26**, 5265-5275.
Nagae, S., Tanoue, T. and Takeichi, M. (2007). Temporal and spatial expression profiles of the Fat3 protein, a giant cadherin molecule, during mouse development. *Dev. Dyn.* **236**, 534-543.

Napoletano, F., Occhi, S., Calamita, P., Volpi, V., Blanc, E., Charroux, B., Royet, J. and Fanto, M. (2011). Polyglutamine Atrophin provokes neurodegeneration in Drosophila by repressing fat. *EMBO J.* **30**, 945-958.
Ponassi, M., Jacques, T. S., Ciani, L. and ffrench Constant, C. (1999). Expression of the rat homologue of the Drosophila fat tumour suppressor gene. *Mech. Dev.* **80**, 207-212.
Qian, D., Jones, C., Rzadzinska, A., Mark, S., Zhang, X., Steel, K. P., Dai, X. and Chen, P. (2007). Wnt5a functions in planar cell polarity regulation in mice. *Dev. Biol.* **306**, 121-133.
Rock, R., Schrauth, S. and Gessler, M. (2005). Expression of mouse dchs1, fjx1, and fat-j suggests conservation of the planar cell polarity pathway identified in Drosophila. *Dev. Dyn.* **234**, 747-755.
Saburi, S. and McNeill, H. (2005). Organising cells into tissues: new roles for cell adhesion molecules in planar cell polarity. *Curr. Opin. Cell Biol.* **17**, 482-488.
Saburi, S., Hester, I., Fischer, E., Pontoglio, M., Eremina, V., Gessler, M., Quaggin, S. E., Harrison, R., Mount, R. and McNeill, H. (2008). Loss of Fat4 disrupts PCP signaling and oriented cell division and leads to cystic kidney disease. *Nat. Genet.* **40**, 1010-1015.
Sah, V. P., Attardi, L. D., Mulligan, G. J., Williams, B. O., Bronson, R. T. and Jacks, T. (1995). A subset of p53-deficient embryos exhibit exencephaly. *Nat. Genet.* **10**, 175-180.
Sang, L., Miller, J. J., Corbit, K. C., Giles, R. H., Brauer, M. J., Otto, E. A., Baye, L. M., Wen, X., Scales, S. J., Kwong, M. et al. (2011). Mapping the NPHP-JBTS-MKS protein network reveals ciliopathy disease genes and pathways. *Cell* **145**, 513-528.
Shen, Y., Lee, G., Choe, Y., Zoltewicz, J. S. and Peterson, A. S. (2007). Functional architecture of atrophins. *J. Biol. Chem.* **282**, 5037-5044.
Simon, M. A., Xu, A., Ishikawa, H. O. and Irvine, K. D. (2010). Modulation of fat:dachsous binding by the cadherin domain kinase four-jointed. *Curr. Biol.* **20**, 811-817.
Simons, M. and Mlodzik, M. (2008). Planar cell polarity signaling: from fly development to human disease. *Annu. Rev. Genet.* **42**, 517-540.
Skouloudaki, K., Puetz, M., Simons, M., Courbard, J. R., Boehlke, C., Hartleben, B., Engel, C., Moeller, M. J., Englert, C., Bollig, F. et al. (2009). Scribble participates in Hippo signaling and is required for normal zebrafish pronephros development. *Proc. Natl. Acad. Sci. USA* **106**, 8579-8584.
Stottmann, R. W., Berrong, M., Matta, K., Choi, M. and Klingensmith, J. (2006). The BMP antagonist Noggin promotes cranial and spinal neurulation by distinct mechanisms. *Dev. Biol.* **295**, 647-663.
Stuebner, S., Faus-Kessler, T., Fischer, T., Wurst, W. and Prakash, N. (2010). Fzd3 and Fzd6 deficiency results in a severe midbrain morphogenesis defect. *Dev. Dyn.* **239**, 246-260.
Tanoue, T. and Takeichi, M. (2004). Mammalian Fat1 cadherin regulates actin dynamics and cell-cell contact. *J. Cell Biol.* **165**, 517-528.
Tanoue, T. and Takeichi, M. (2005). New insights into Fat cadherins. *J. Cell Sci.* **118**, 2347-2353.
Van Hateren, N. J., Das, R. M., Hautbergue, G. M., Borycki, A. G., Placzek, M. and Wilson, S. A. (2011). FatJ acts via the Hippo mediator Yap1 to restrict the size of neural progenitor cell pools. *Development* **138**, 1893-1902.
Viktorinova, I., Konig, T., Schlichting, K. and Dahmann, C. (2009). The cadherin Fat2 is required for planar cell polarity in the Drosophila ovary. *Development* **136**, 4123-4132.
Wang, J., Hamblet, N. S., Mark, S., Dickinson, M. E., Brinkman, B. C., Segil, N., Fraser, S. E., Chen, P., Wallingford, J. B. and Wynshaw-Boris, A. (2006). Dishevelled genes mediate a conserved mammalian PCP pathway to regulate convergent extension during neurulation. *Development* **133**, 1767-1778.
Wang, Y., Thekdi, N., Smallwood, P. M., Macke, J. P. and Nathans, J. (2002). Frizzled-3 is required for the development of major fiber tracts in the rostral CNS. *J. Neurosci.* **22**, 8563-8573.
Wang, Y., Guo, N. and Nathans, J. (2006). The role of Frizzled3 and Frizzled6 in neural tube closure and in the planar polarity of inner-ear sensory hair cells. *J. Neurosci.* **26**, 2147-2156.
Wright, K. M., Vaughn, A. E. and Deshmukh, M. (2007). Apoptosome dependent caspase-3 activation pathway is non-redundant and necessary for apoptosis in sympathetic neurons. *Cell Death Differ.* **14**, 625-633.
Yamamoto, N., Okano, T., Ma, X., Adelstein, R. S. and Kelley, M. W. (2009). Myosin II regulates extension, growth and patterning in the mammalian cochlear duct. *Development* **136**, 1977-1986.
Yanagisawa, H., Bundo, M., Miyashita, T., Okamura-Oho, Y., Tadokoro, K., Tokunaga, K. and Yamada, M. (2000). Protein binding of a DRPLA family through arginine-glutamic acid dipeptide repeats is enhanced by extended polyglutamine. *Hum. Mol. Genet.* **9**, 1433-1442.
Yang, C. H., Axelrod, J. D. and Simon, M. A. (2002). Regulation of Frizzled by fat-like cadherins during planar polarity signaling in the Drosophila compound eye. *Cell* **108**, 675-688.
Yates, L. L., Papakrivopoulou, J., Long, D. A., Goggolidou, P., Connolly, J. O., Woolf, A. S. and Dean, C. H. (2010). The planar cell polarity gene Vangl2 is required for mammalian kidney-branching morphogenesis and glomerular maturation. *Hum. Mol. Genet.* **19**, 4663-4676.
Yu, H., Smallwood, P. M., Wang, Y., Vidaltamayo, R., Reed, R. and Nathans, J. (2010). Frizzled 1 and frizzled 2 genes function in palate, ventricular septum and neural tube closure: general implications for tissue fusion processes. *Development* **137**, 3707-3717.
Yu, J., Ying, M., Zhuang, Y., Xu, T., Han, M., Wu, X. and Xu, R. (2009). C-terminal deletion of the atrophin-1 protein results in growth retardation but not neurodegeneration in mice. *Dev. Dyn.* **238**, 2471-2478.
Zoltewicz, J. S., Stewart, N. J., Leung, R. and Peterson, A. S. (2004). Atrophin 2 recruits histone deacetylase and is required for the function of multiple signaling centers during mouse embryogenesis. *Development* **131**, 3-14.